The Mason Project Presents

The S.T.O.R.K.

An Inter-Theater Tactical Transport with Austere STOL Capability

2006-2007 AIAA Undergraduate Team Design Competition

Virginia Polytechnic Institute & State University
Aerospace and Ocean Engineering Department
Blacksburg, Virginia

May 7, 2007

Aisley Neary
246790

Mark Gabbard
278802

Craig Searles
246831

Taylor Raymond
246791

Alexander Simpson
247275

Adam Reardon
278800

David Macdonald
274347

Robert Speer
246736

Michael Hazuda
275320

Yaman Atici
281886

Table of Contents

Table of Figures

Table of Tables

Nomenclature

Symbol	*Definition*
a_s	Lift Curve Slope of Stabilizer
a_w	Lift Curve Slope of Wing
AR	Aspect Ratio
A_u	Required Area
b	Wing Span
C_{bar}	Mean Chord
C_{bleed}	Bleed Correction Factor
C_D	Drag Coefficient
C_{D0}	Zero Lift Drag
C_{Di}	Induced Drag
$C_{DL\&P}$	Leakages
$C_{D_{misc}}$	Drag Coefficient of various parts of the aircraft
$C_{D_{trim}}$	Trim Drag
C_d	Section Drag Coefficient
C_{fc}	Flat Plate Skin Friction
C_L	Lift Coefficient
C_{L_α}	Lift Slope
C_l	Section Lift Coefficient
C_{L_t}	Lift Coefficient on the Tail
C_{L_F}	Lift Coefficient for the Free Stream
C_m	Moment Coefficient
$C_{m_{ac_{wb}}}$	Coefficient of Moment about the ac for the Wing Body
C_{m_p}	Moment Coefficient of the Propulsive System
C_n	Yawing Moment Coefficient
C_{n_β}	Weathercock Stability Derivative
$C_{n_{\delta r}}$	Yawing Moment Coefficient with Respect to Rudder Deflection
C_{n_T}	Yawing Moment with Respect to Thrust
C_r	Root Chord
C_{ram}	Ram Recovery Correction Factor
C_t	Tip Chord
d	Fuselage Diameter
$\frac{d\varepsilon}{d\alpha}$	Change in Stabilizer ε versus change in wing α
ε	Downwash Angle

e	Oswald Efficiency Factor
F	Fuselage Lift Factor
FF_c	Form Factor
GCR	Climb Gradient
h_n	Neutral Point
h_o	Aerodynamic Center of the wing
$(h - h_{n_{wb}})$	Negative difference in static margin
K_n	Static Margin
L/D	Lift to Drag Ratio
l_F	Distance from the cg over the wing to the cg of the vertical tail
l_t	Distance between the ac of the wing and horizontal tail
M	Mach
M_{DD}	Divergence Mach Number
M_y	Local Moment
N	Number of Engines
η_s	Stabilizer Efficiency
$\left(\frac{P_1}{P_0}\right)_{actual}$	Actual Pressure Ratio
$\left(\frac{P_1}{P_0}\right)_{ref}$	Reference Pressure Ratio
Q_c	Interference Factor
q	Dynamic Pressure
S	Planform Area of the wing
S_a	Obstacle Length
S_F	Free Stream Surface Area
S_{land}	Landing Distance
S_t	Planform Area of the Horizontal Tail
S_{tofl}	Take off Field Length
T	Thrust
t	Airfoil Thickness
t/c	Thickness to Chord Ratio
T/W	Thrust to Weight Ratio
TOP	Take Off Parameter
V	Airspeed
V_F	Vertical Tail Volume Ratio
$\overline{V}_H$	Horizontal Tail Volume Ratio
V_s	Stabilizer Volume Coefficient
W	Weight

W_o	Total Weight
W_{crew}	Crew Weight
$W_{fixedpayload}$	Fixed Payload Weight
$W_{droppedpayload}$	Dropped Payload Weight
W_f	Fuel Weight
W_{fi}	Individual Mission Segment Fuel Consumption
W_e	Empty Weight
W_{1-11}	Weights for Individual Mission Segments
W/S	Wing Loading
x	Locations
y_p	Lateral distance to the line of action of thrust
z_p	Distance between the vertical cg location and the thrust line

Greek

α	Angle of Attack
β	Slide Slip Angle
δ_r	Rudder Deflection
Λ	Sweep
λ	Taper Ratio
ρ	Density
σ_u	Ultimate Stress

Abbreviations

AIAA	American Institute for Aeronautics and Astronautics
AoA	Angle-of-Attack
AC	Aerodynamic Center
CBR	California Bearing Ratio
CG	Center-of-Gravity
FBW	Fly-by-Wire
FDAV	Future Deployable Armored Vehicle
GPS	Global Positioning System
HF	High Frequency
HUD	Heads Up Display
MAC	Mean Aerodynamic Chord
RFP	Request for Proposal
STOL	Short Take Off and Landing
UHF	Ultra High Frequency
USAF	United States Air Force
USB	Upper Surface Blowing
VHF	Very High Frequency

1. Introduction

As fighting intensifies around the world, the US continues to send aid, in the form of troops, to stricken areas in the hopes of defending and improving the lives of innocents. It is therefore necessary for the military to provide these troops with the best technology to aid in the fighting. The American Institute for Aeronautics and Astronautics (AIAA) describes in their RFP, a need for tactical warfare mobility to be utilized by the United States Air Force (USAF). The USAF is particularly in need of inter theater transports with austere STOL capabilities to supply ground troops with Future Deployable Armored Vehicles (FDAV's) and equipment, as well as provide reconnaissance for commanders worldwide.

In this report, the next generation of tactical transport is presented in the form of the S.T.O.R.K. by The Mason Project. Based on available analysis and careful calculations, the S.T.O.R.K., shown in Figure 1.1 is a viable solution to the proposal set forth by the AIAA for the 2006-2007 Undergraduate Design Competition.

Figure 1.1 The S.T.O.R.K.

2. Understanding the Problem

The request for proposals (RFP) put forth by the AIAA for 2006-2007[1] calls for an inter-theatre tactical transport with austere STOL capabilities which shall be capable of performing two distinct missions for the United States Air Force. The design mission requires the craft to transport a payload, therefore commanding the initial sizing parameters, while the ferry mission requires the craft to have a large range, which takes precedence over the lift characteristics.

2.1. Design Mission

The Design Mission calls for the aircraft to transport a Future Deployable Armored Vehicle (FDAV) over a distance of greater than 1,000 nautical miles. The FDAV weighs 25 tons, with an additional 5 tons required for support equipment. A one foot escape path is needed around the FDAV, which has dimensions of 560" long by 128" wide by 114" high, and a crew of 3 must be accounted for in the sizing parameters for the cockpit. The transport must be able to warm-up and taxi for 8 minutes before taking off from a balanced field length of less than 2,500 ft, and then take off under "combat rules" which define clearing a 50 ft obstacle at the end of the runway. The flight path for this mission can be seen in Figure 2.1. It must then climb to best cruise altitude for 500 nm at a speed greater than or equal to $M = 0.8$ before descending to 1000 ft for 100 nm at a speed of $M = 0.6$. The transport must then descend to sea level, land and deliver the FDAV, and mirror the outbound mission on return.

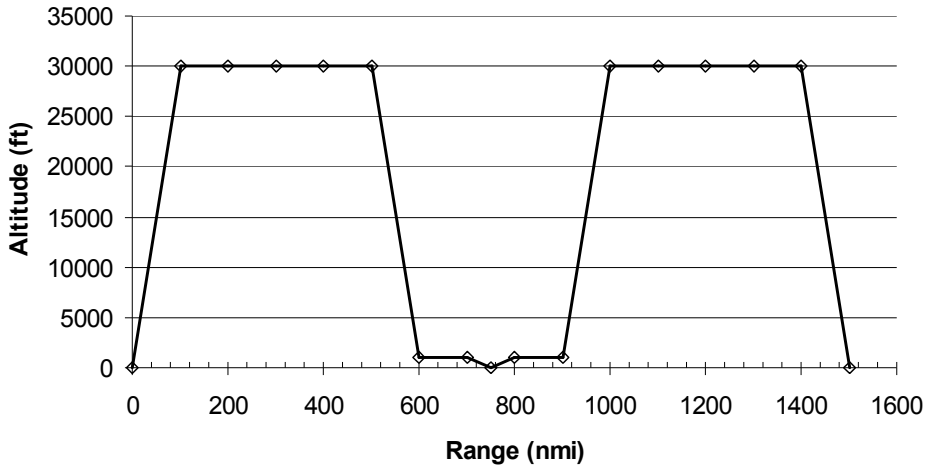

Figure 2.1: Design mission flight path

After turning around and mirroring the outbound mission, it must then land within 2,500 ft on a landing zone of CBR 4-6 with the possibility of a 25 knot crosswind with a 5 knot tailwind component. The fuel consumption considerations must include using a takeoff fuel allowance of 2 minutes of operation at maximum takeoff power. The critical design parameters for this mission are the size of the cargo area, and the ability to cruise at the required speed.

2.2. Transoceanic Ferry Mission

The Ferry Mission requires no additional payload for the transport, but instead demands the ability to fly a range of over 3200 nm. The craft must again warm-up and taxi for 8 minutes before taking off within 2,500 ft over a 50 ft obstacle. It must then cruise to best altitude at a speed of greater than or equal to $M = 0.8$ for a distance of 3,200 nm before descending to sea level to conduct a normal approach to runway of 2,500 ft or less and a balanced field length of 2,000 ft. The mission concludes with a taxi into the gate and parking at idle power for 10 minutes. The reserve fuel must be enough such that the aircraft could accommodate a missed approach with 150 nm diversion, along with a 45 minute holding pattern at 5,000 ft. The essential consideration with this mission is the fuel allowance, and number of in-flight refueling needed to complete the mission.

Some of the main problems posed by the RFP were those of speed and endurance. For the design mission, the S.T.O.R.K. must carry a nominal load of 30 tons at a speed of $M \geq 0.8$. While similarly sized aircraft such as the Lockheed C-130 Hercules and the Boeing YC-14 were created for transport and had STOL capabilities, they only had maximum cruise speeds of approximately $M = 0.448$[2] and $M = 0.662$[3] respectively. This meant that in sizing the S.T.O.R.K., the limitations of current transport must be overcome to design for the future. For the ferry mission, the S.T.O.R.K. proves itself worthy for long-range reconnaissance means, and stays airborne at cruise speed for 3,200 nautical miles, which was much further than either the C-130 at 2,050 nm or the YC-14 at 2,770 nm. As the requirements set by the RFP were above and beyond aircraft today, The Mason Project knew that the S.T.O.R.K. needed to add innovation to convention to find a solution to meet the needs of today's Air Force. Table 2.1 below is a listing of the requirements as posed in the RFP, showing that the S.T.O.R.K. adequately meets the desired specifications.

Table 2.1 Requirements Summary

RFP Requirement	Accomplished
Design Mission	
Carry Future Deployable Armored Vehicle	✓
Carry Crew of 3 (Pilot, Copilot, Loadmaster)	✓
Takeoff with balanced field length <2,500ft on hot day (95°F)	✓
Cruise 600 nm at Mach 0.8 according to prescribed profile (no refueling)	✓
Land with balanced field length <2,500ft (25 knot crosswind, 5 knot tailwind component)	✓
Takeoff under combat rules in <2,500ft	✓
Mirror outbound profile for return to base (no refueling)	✓
Ferry Mission	
Carry 10 tons of bulk cargo	✓
Carry Crew of 3 (Pilot, Copilot, Loadmaster)	✓
Takeoff with balanced field length <2,500ft on hot day (95°F)	✓
Cruise 3200 nm at Mach 0.8 at best cruise altitude (with refueling)	✓
Land with balanced field length <2,500ft	✓
Reserve fuel for missed approach, 150 nm diversion, and 45 min hold at 5,000 ft	✓

3. Evolution, Selection, Description

At the beginning of the design process, eight sketches were put forth by members of The Mason Project for consideration in this competition. The original designs included everything from basic transport aircraft modeled after current transports, strut-braced designs, mid- and high-wing placements, two and four engine configurations, bi-wing concepts, blended wing-body concepts, and both upper and lower wing-surface mounted engines. One view of each of the initial sketches of these designs can be seen in Figure 3.1-3.8 below, and full views can be seen in Figures A.1 through A.8. These designs were then evaluated in terms of the requirements in the RFP.

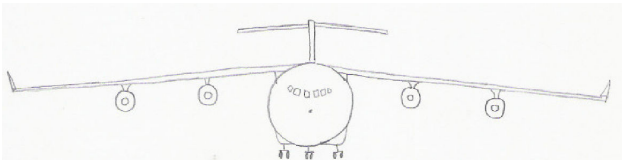

Figure 3.1 Initial Sketch 1

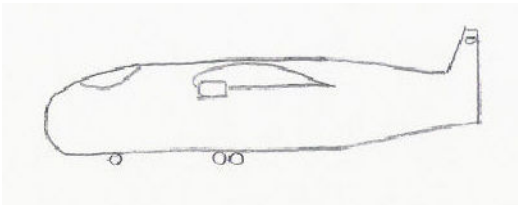

Figure 3.2 Initial Sketch 2

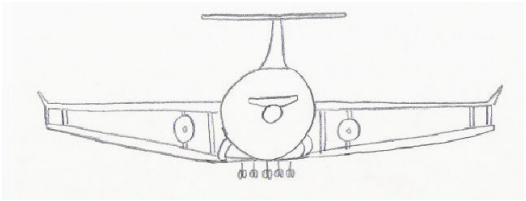

Figure 3.3 Initial Sketch 3

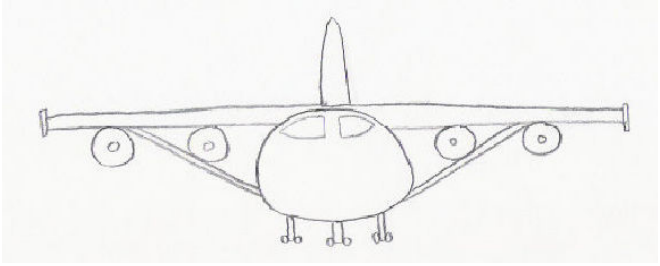

Figure 3.4 Initial Sketch 4

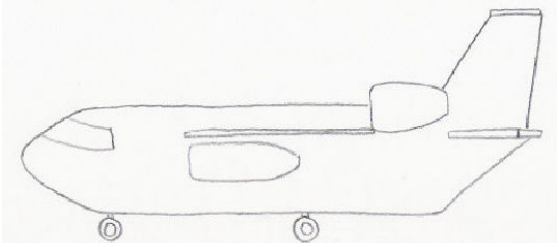

Figure 3.5 Initial Sketch 5

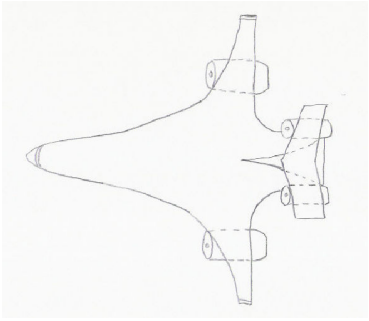

Figure 3.6 Initial Sketch 6

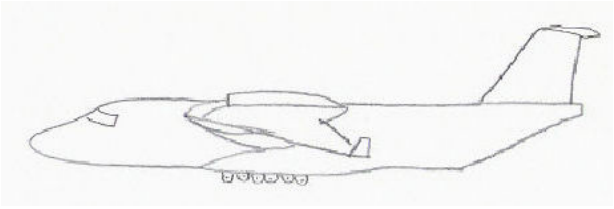

Figure 3.7 Initial Sketch 7

Figure 3.8 Initial Sketch 8

A decision matrix was formed based on the most important requirements as determined by The Mason Project. As seen in Table 3.1, the design parameters which were the most important were accomplishing the RFP requirements, and feasibility of design. The next two factors of equal weight were the ability to achieve a large amount of lift and obtaining the desired cruise speed. These first four factors were very important to The Mason Project as without high totals for these aspects, any design would not be acceptable for submission in this competition. Having a low weight and being capable of performance in austere conditions were the next considerations which taken into account. With lower structural weight, the aircraft can store more cargo and fuel, which is beneficial for both the design and ferry missions in the RFP. The amount of innovation which went into the design was the next factor to be graded. While convention is a good starting point, new technologies come about through innovation and creativity. The amount of originality which went into each design showed the ability of The Mason Project group members to think outside of the proverbial box and find new ways to support our troops. The factors which contributed the least to the overall score for each design were those of maintenance, cost and marketability. After reviewing the eight designs, the amount of maintenance required, and the ease of maintenance was seen to be a factor which could help define which designs would make it to the next phase of the design process. The total cost was something which was estimated for this decision matrix, as initially in the design phase, the cost could be accurately calculated. Designs which appeared to cause a rise in cost due to unusual shape, or excess design parameters were given a low point value, and those which were thought of as easier to manufacture and maintain were given a higher point value. The last decision on this matrix was the marketability of the craft. An original design poses both pros and cons for its marketability. If a design is too unusual or modern, a client may be unlikely to pursue a purchase as it is unfamiliar. However, if a design is too similar to transports readily available on the market, they may also not pursue a contract as they are looking for innovation in a new design. A proper amount of artistic design must be considered to make it marketable, and so the sketches which were the most visually appealing earned the highest points in this category.

Table 3.1 Decision Matrix

Factor	**Pt. Value**	**1**	**2**	**3**	**4**	**5**	**6**	**7**	**8**
Accomplish Requirements	18	**15**	15	14	10	13	**15**	**15**	14
Feasibility	15	**15**	12	7	10	12	**11**	**12**	9
High Lift Ability	12	**9**	4	10	9	6	**9**	**10**	12
High Cruising Speed	12	**9**	6	6	7	10	**12**	**9**	8
Low Weight	9	**7**	7	5	7	6	**7**	**8**	7
Austere Capabilities	9	**8**	7	6	6	5	**4**	**8**	7
Innovation	8	**4**	2	7	5	4	**8**	**6**	6
Maintenance	7	**7**	5	4	6	5	**6**	**5**	2
Low Cost	5	**5**	5	2	3	4	**3**	**5**	3
Marketability	5	**5**	4	3	4	4	**4**	**5**	3
Totals:	100	**84**	67	64	67	69	**79**	**83**	71

Once the totals were calculated, sketches 1, 6, and 7 were chosen based on their point values. Each design earned high marks in the first, and most important, four factors of accomplishing requirements, feasibility, high lift ability, and high cruising speed. Design 1 earned highest marks for maintenance due to the location of critical components. Design 6 performed well in high cruising speed, as its blended-wing-body concept allowed for a greater wing surface area. Design 7 seemed the safest for low weight and austere capabilities, with its simple design and upper-surface mounted engines.

These three designs can be classified simply as 1) a pod-mounted high wing design, 2) a blended wing body design, and 3) a high-wing design. Two common factors through these designs were a high T-tail, along with aft-swept wings, both of which were carried through into the S.T.O.R.K. The decision to adopt the pod-mounted wings came from the need for the transport to operate in austere conditions. While in this competition the landing surface is known, pilots in the field may have to land on uneven surfaces potentially filled with debris. By incorporating engines mounted on the upper surface of the wing, the possibility of damage due to

debris was minimized. Another benefit of upper surface pod-mounted engines is the effect of upper surface blowing over the wing. This natural airflow over the trailing edge from the engine exhaust, along with airflow on the lower surface of the wing through bleed air from the engine aids in lift during take-off, allows for slower landing speeds. The strut-braced concept was then incorporated due to the realization that, with such a design, the wing could be longer, thinner, and lighter, all parameters which would eventually aid in driving down cost, as well as weight.

4. Constraint Diagram/Initial Sizing

To properly size the S.T.O.R.K., the Mason Project initially looked at similarly sized military transport aircraft to gain a baseline idea of sizes. The Lockheed C-130, Boeing C-17, Airbus A400, and Lockheed C-5 possessed characteristics and specifications near those which were required in this competition. Concurrently, the Mason Project began creating a constraint diagram, Figure 4.1, which compared the thrust to weight ratio and the wing loading to determine the design parameters. To plot the line that relates the W/S and T/W for cruise, the following equation was used:

$$\left(\frac{T}{W}\right) = q * \frac{C_{d0}}{W/S} + \frac{W/S}{q\pi Ae} \tag{4.1}$$

The dynamic pressure for M = 0.8, an aspect ratio of 10.74, and an estimated Oswald efficiency factor of 0.95 were used in equation 4.1. The red line in Figure 4.1 below represents the cruise conditions. The green line represents the relation of *T/W* and *W/S* for takeoff. The thrust to weight required at takeoff for a given wing loading was dictated by the equation below:

$$\frac{T}{W} = \frac{(TOP) * W/S}{\sigma C_{Lmac} s_{tofl}} \tag{4.2}$$

The takeoff parameter (*TOP*) was determined to be 65 from a graph on page 99 in Raymer's book. The blue line in the constraint diagram represents the thrust to weight ratio for the climb gradient. It is represented by the equation below:

$$\frac{T}{W} = \left(\frac{N}{N-1}\right)\frac{CGR - 1}{L/D} \tag{4.3}$$

The number of engines, N, was 4 and the climb gradient used was 0.03, while the lift to drag ratio was 14.1. The cyan line represents the wing loading required for landing. It was determined by the equation below:

$$W/S = \frac{(S_{land} - S_a)}{80\sigma C_{L\max}} \tag{4.4}$$

Using a landing distance of 2500 ft and an obstacle length S_a to be 450 ft, the result was found to be a wing loading of 118 lbs/ft^2. The solution set was found to be above the green and

red lines and to the left of the landing constraint. An estimated wing loading was determined to be approximately 0.7 based on the evaluation of similar planes aircraft. For that *T/W*, it was decided to use a wing loading of around 107 lbs/ft^2. The design point for the S.T.O.R.K. was not at the matched point of our constraint diagram because it was felt that additional thrust would be needed to take off and cruise at Mach 0.8. The S.T.O.R.K. was chosen to be in the solution set but not precisely at any of the constraint lines so that room to change was available.

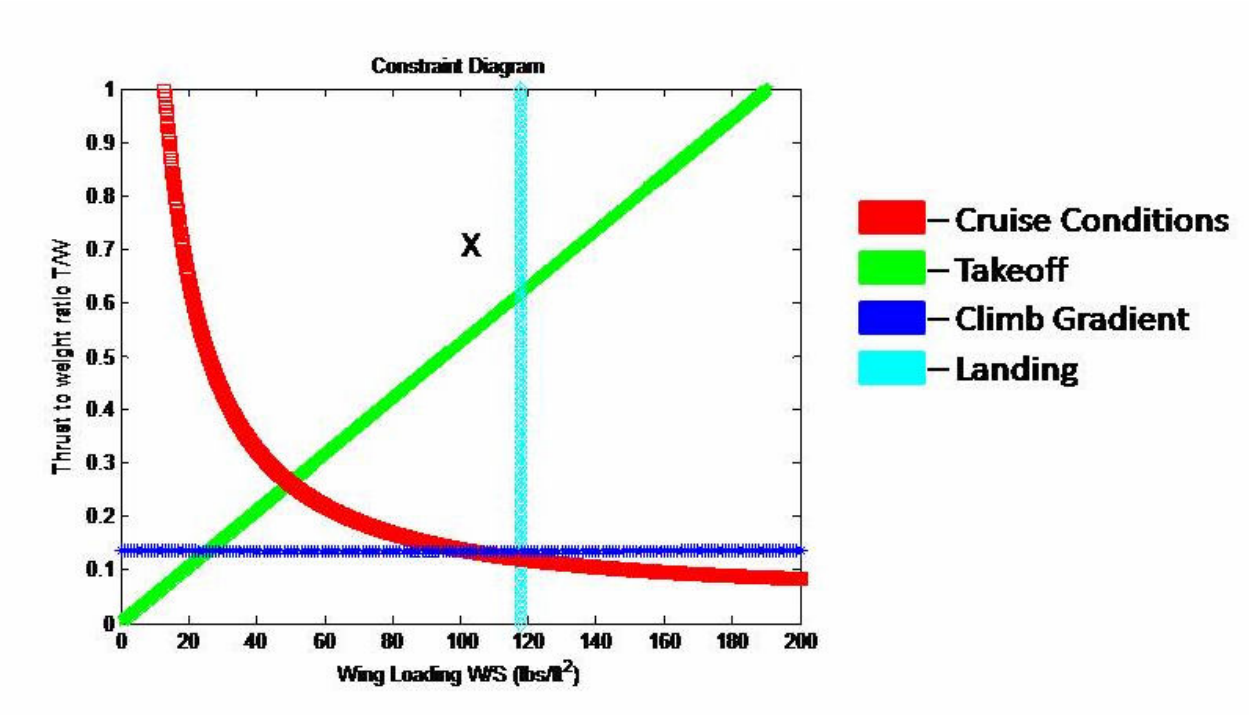

Figure 4.1 Constraint Diagram

5. The S.T.O.R.K.

Once the S.T.O.R.K. was selected as the concept of choice, a three-dimensional drawing was needed to better visualize the concept. As the concept evolved, the initial concept changed. A strut frame was chosen to lighten the wing structure so that the wingspan could be increased from the initial 100 ft to the final 145 ft. This helped to create more volume available for fuel storage, as well as higher lift coefficients at lower speeds.

The wing position was pushed further aft to better balance the aircraft as the original placement of the wing caused the CG to be too far from the AC to maintain stability. This is displayed in the progression from Figure 5.1 to Figure 5.2.

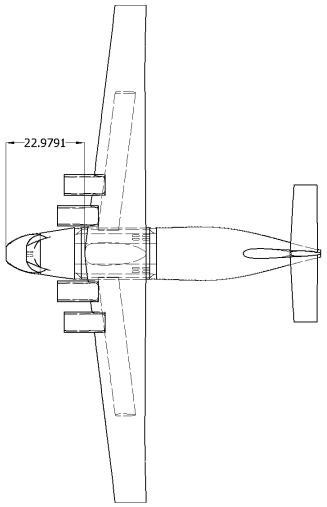

Figure 5.1 Original Wing Location

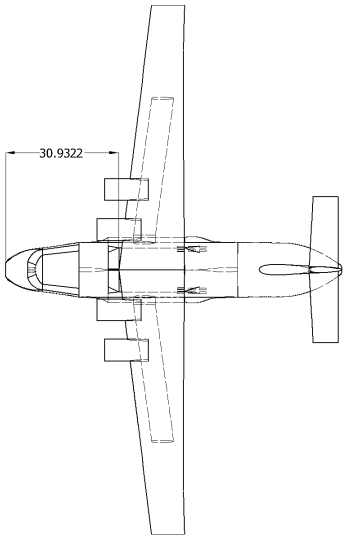

Figure 5.2 New Wing Location

The wing's shape was altered at this point to its final form, as shown in Figure 5.3. The positions and sizes of the control/high lift surfaces can also be seen below.

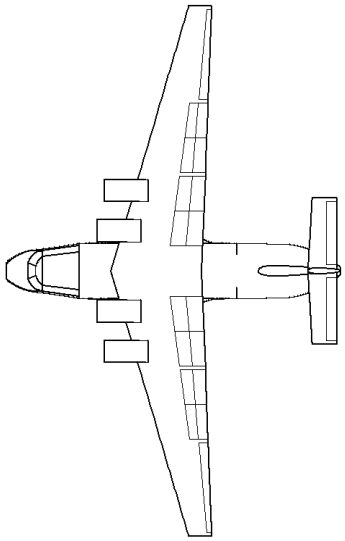

Figure 5.3 Final Wing Location and Configuration

The wing is mounted on top of the fuselage, as having a high wing allows the fuselage to be closer to the ground, making loading and unloading of the cargo easier, which will be loaded and

unloaded via a ramp. The strut is tied into the bulkheads for the landing gear on the fuselage, and the strut extends to 65% of each wing semi span. As the structure at that location already needs to have a significant amount of strength, this was the most logical choice for the connection point on the aircraft.

The S.T.O.R.K. has 4 engines, two on each wing. The center of the first engine is located 11 feet from centerline, and the second engine is located 20 feet from centerline. These locations were chosen to account for an engine out situation. The engine position also allows the engine to be lowered straight to the ground for ease in engine change and maintenance. The engines are mounted such that the exhaust will blow over the upper surface of the wing and flaps. This will provide the powered lift necessary to achieve the STOL requirements.

A high T-tail design was incorporated into the S.T.O.R.K. The span of the horizontal tail is 40 ft with a horizontal stabilizer, and it has a tip chord of 7 feet. The tail extends 20 feet above the fuselage, which has a maximum width of 15.6 feet, is 92 feet long, and 15 feet high. These were the best dimensions to add for the placement of the payload. A high T-tail was chosen to keep the tail outside the wing wash, allowing for smaller control surfaces.

The landing gear chosen was a triangle type. The lengthwise wheel base was increased to 87 feet from the initial 36 feet. The two nose gear wheels remained the same, while the eight rear wheels were increased to twelve, six on either side of the fuselage. The tip back angle was increase from seven degrees to sixteen degrees to facilitate shorter takeoffs and landings as shown in Figures 5.4 and 5.5. The widthwise wheel base was expanded from 11 feet to 13 feet by growing the landing gear pods displayed in Figures 5.6 and 5.7.

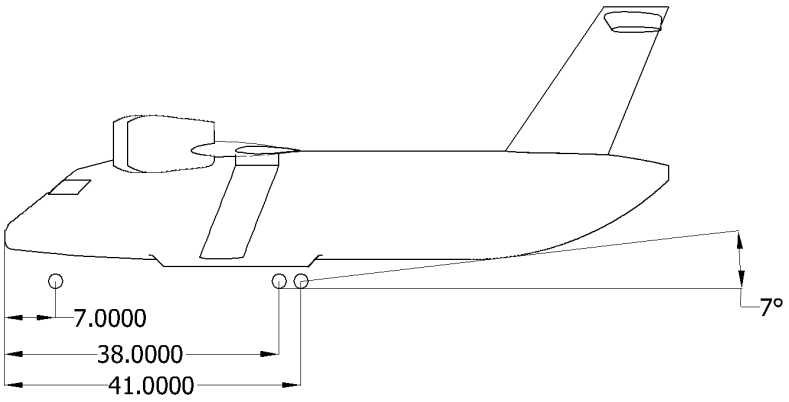

Figure 5.4 Initial Landing Gear Configuration and Tail Scrape Angle

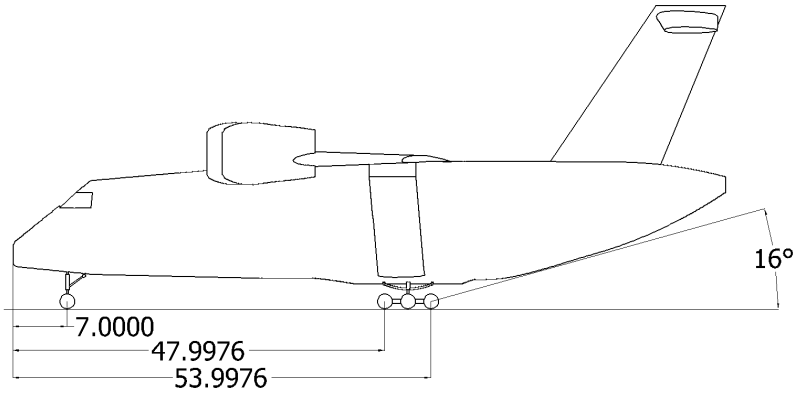

Figure 5.5 Final Configuration

Also seen in Figures 5.6 and 5.7, the wing-fuselage junction was squared off to reduce aerodynamic interference.

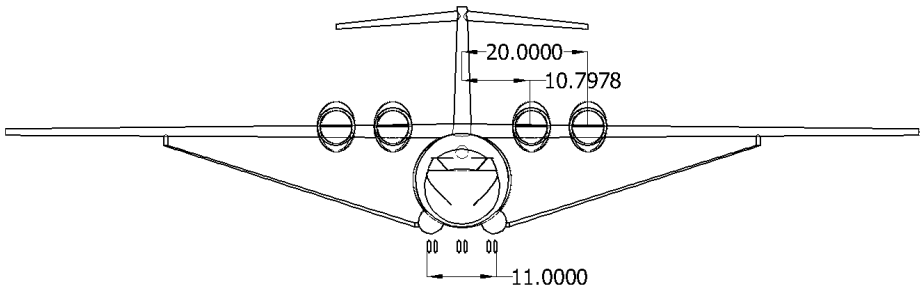

Figure 5.6 Initial Configuration

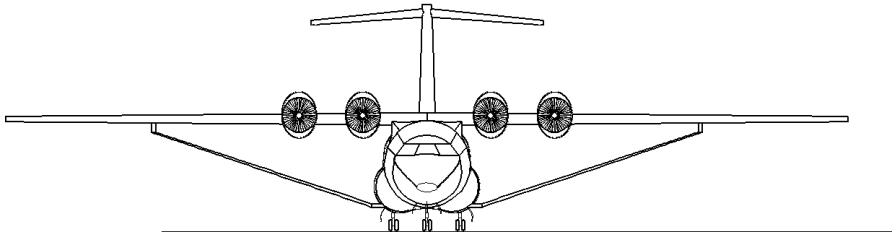

Figure 5.7 Final Configuration

6. Crew Station Layout

When coming up with a layout for the crew stations, there were a few constraints that needed to be taken into account. The initial consideration was that the cargo bay area needed to be maximized and not constrained. Since the most amount of room is needed for FDAV, the storage space and lavatory would be placed on the forward port and starboard sides of the aircraft. They would fit behind the cockpit but forward of the main cargo bay. With the general placement of the compartments decided, the type of access to the crew station and cockpit needed to be determined. There were two different types of entry ways which were found to be the most feasible. The first that was considered was a staircase, Figure 6.1, which would lead from the floor of the cargo bay to the floor of the crew stations.

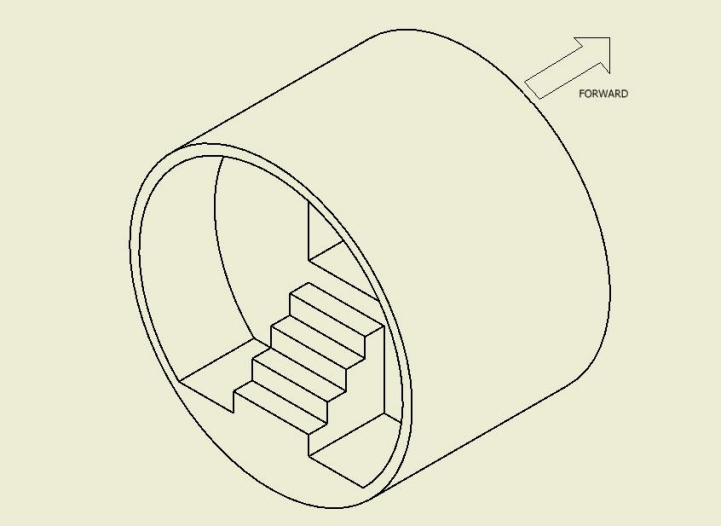

Figure 6.1 Stair Entrance Option

The second option was to use a ladder to climb up into the crew station/cockpit area. Considering the height of the floor of the crew station from the bottom of the plane, the stairwell could extend into the cargo bay taking up space that could be used for other more important items. With that in mind, the best option would be a ladder, Figure 6.2.

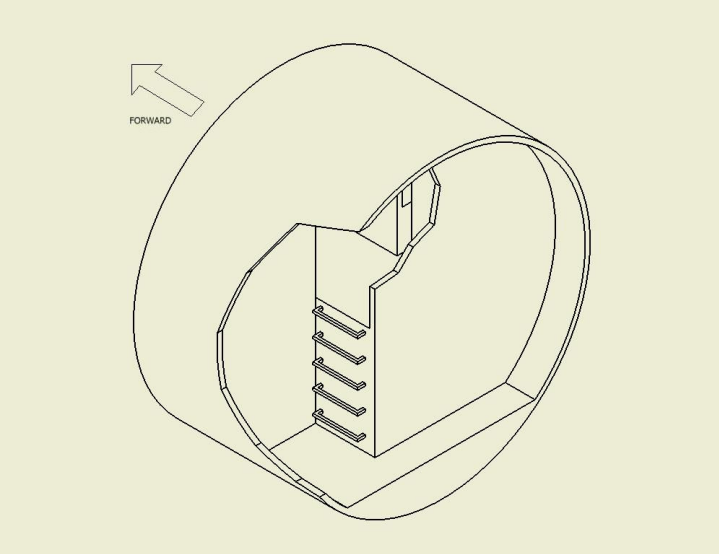

Figure 6.2 Ladder Entrance Option

A ladder allows for the most amount of space that can be used for cargo, and also allows for more freedom with the layout of compartments for the crew.

The placement of the compartments, lavatory and storage, was straightforward. The lavatory was placed on the starboard side of the fuselage and the storage/galley compartment opposite it, on the port side. The next problem that had to be dealt with was where to place the loadmaster's seat. The initial design had the loadmaster sitting rear of the lavatory facing the port side of the fuselage, opposite the ladder. Even though the loadmaster would be closer to the cargo in that position, a spot nearer to the pilot and co-pilot was eventually decided upon. The reason behind his chair placement, off to the starboard side of the fuselage, was to make it easier for the pilot and co-pilot to enter and exit their seats. That would also result in more space for the crew stations and would allow them to be placed as far forward to maximize the cargo bay area.

7. Cargo Bay Layout

The initial design for the fuselage was constrained to fit around the FDAV, but the cargo bay area would be useless without an efficient means of loading and unloading. Allowing the cargo bay door to be opened through two doors which open outwards, both up and down will create a more efficient loading and unloading area. Figure 7.1 shows a 3-view drawing of the cargo bay area doors.

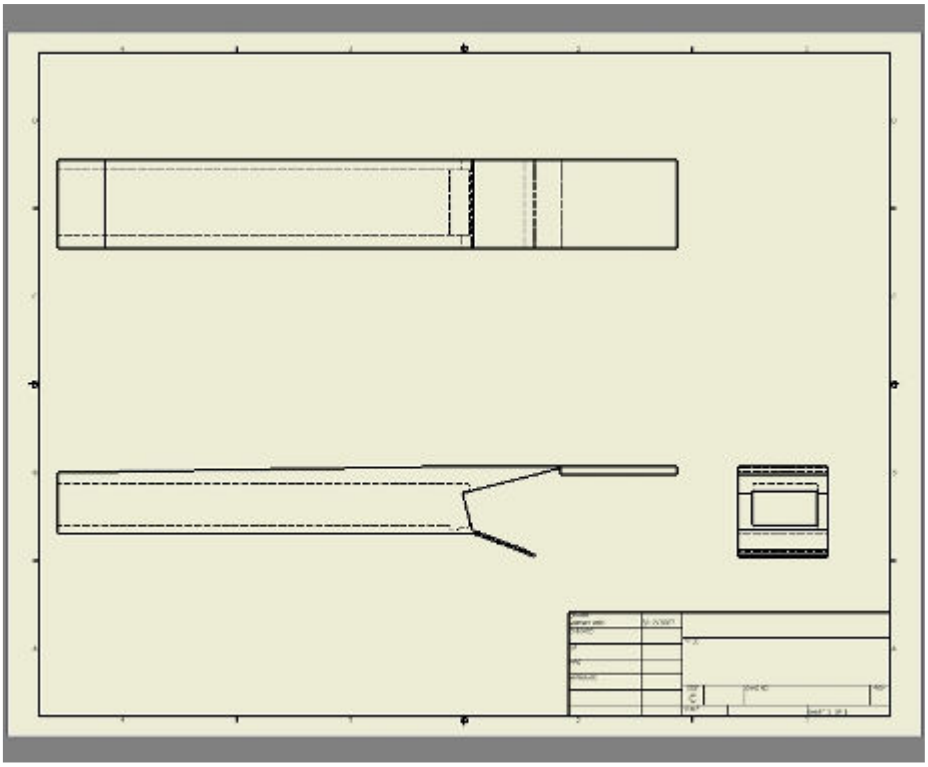

Figure 7.1 Cargo Bay Layout

As shown above cargo bay doors open both ways while one goes up the other one goes down which creates an efficient loading/unloading potential. For easier loading, the bottom door extends completely to the ground, at an angle of 15 degrees. The estimated length is 1022 inches an estimation of 216 inches loadable width which is twice the FDAV's size.

The other possible option for the cargo bay door was to make the whole door slide down but with that option, the door would encounter more tension so we would need more material to keep it strong enough to carry the given vehicle.

8. Weights

The weight estimation for the aircraft was performed using equations from chapter 6 in Raymer's book. This method used an initial guess of the total weight to calculate a new weight. A new weight is guessed from the range of values between the original estimations and the calculations; iterations are made until the initial estimation and the calculated value are within a few percentages of one other.

The original weight estimation was made using a growth factor of 3.333; furthermore, the initial guess was 200000 lbs, which was 60000 lbs multiplied by the growth factor. For both of the missions, this was a reasonable growth factor, and the beauty of this iterative method is that regardless of the inaccuracy of the first guess, more iterations are made and the numbers become more accurate. Fortunately, the original weight estimation was very similar to the first calculation, and we gladly took the calculated take off gross weight of 210547 lbs. The mission segments and their respective weight fractions are shown in the table below.

Table 8.1 Mission Segments and Weight Fractions

Segment	Description	Weight Fraction	Mission Segment Fuel (lbs)
0-1	Engine Start, Taxi, Takeoff	0.97	6695.39
1-2	Climb and Accelerate	0.9805	4352.01
2-3	Cruise 1	0.957832	9411.05
3-4	Cruise 2	0.988577	2549.38
4-5	Descent for Landing	0.99	2231.8
5-6	Landing and Taxi back	0.993	1562.26
6-7	Taxi and Takeoff	0.99	2231.8
7-8	Climb and Accelerate	0.9805	4352.01
8-9	Cruise 3	0.949614	11245.1
9-10	Descent for Landing	0.99	2231.8
10-11	Landing and Taxi back	0.992	1785.44
0-13	Total Mission	0.728598	60571.4*

*Note: this fuel weight is higher than the original calculation because the actual weight of 210547 lbs was used in the calculation of the fuel weight instead of the initial guess of 200000 lbs.

The iterative method used to determine these values is shown in the following section. The total weight was calculated from the addition of the weights of the crew, fixed payload, dropped payload, fuel, and empty weight of the aircraft.

$$W_o = W_{\text{crew}} + W_{\text{fixed payload}} + W_{\text{dropped payload}} + W_{\text{fuel}} + W_{\text{empty}} \tag{8.1}$$

This equation was used because all of the weights were known with the exception of the fuel weight. With aerial refueling allowed for the transoceanic ferry mission, the only fuel concern was for the initial delivery of the FDAV. Furthermore, the known quantities were added up to begin the total takeoff weight calculation.

The crew consists of a pilot, copilot, and a loadmaster. Each of the crew is an estimated 200 lbs for a total weight of 600 lbs. The payload is the FDAV, which weighs 25 tons plus 5 tons of support equipment (60000 lbs total). The empty weight fraction was then calculated; this was calculated using the following equation with the constants provided in table 6.1 of Raymer's textbook.

$$\frac{W_e}{W_o} = (a + bW_o^{C1} A^{C2} (T/W_o)^{C3} (W_o/S)^{C4} M_{\max}^{C5}) K_{vs} \tag{8.2}$$

$$\frac{W_e}{W_o} = (0.07 + 1.71(200000lb)^{-0.1} 10.74^{0.1} (150552lb/200000lb)^{0.06} (200000lb/1957.5ft^2)^{-0.1} 0.82^{0.05}) 1.00$$

$$\frac{W_e}{W_o} = 0.462048 \tag{8.3}$$

This calculation was close to the original estimation of 0.5, so initially the errors in the calculations are small.

The total aircraft fuel was all of the fuel used during the mission, plus reserve and trapped fuel. The fuel weight was calculated using the following equation (8.7).

$$W_f = 1.06(\sum_1^x W_{fi}) \tag{8.4}$$

For the engine start, taxi, and takeoff, a reasonable estimate according to Raymer was $\frac{W_1}{W_o} = 0.97$ (8.8).

The climb and accelerate leg of the mission was calculated from another of Raymer equations (8.9).

$$\frac{W_2}{W_1} = 1.0065 - 0.0325M \tag{8.5}$$

$$\frac{W_2}{W_1} = 1.0065 - 0.0325(0.8)$$

$$\frac{W_2}{W_1} = 0.9805$$

Next, the first cruise weight fraction was calculated. This is for cruise at M = 0.8, 30000 ft, for 500nm. The lift to drag ratio used for this calculation was 13.2.

$$\frac{W_3}{W_2} = e^{\frac{-RC}{V(L/D)}} \tag{8.6}$$

$$\frac{W_3}{W_2} = e^{\frac{-500nm\,0.61/hr}{0.8(589.5kts)(13.2)}} \tag{8.7}$$

$$\frac{W_3}{W_2} = 0.957832$$

The second cruise is at 1000 ft for 100nm.

$$\frac{W_4}{W_3} = e^{\frac{-100nm\,0.6/hr}{0.6(659.4kts)(13.2)}} \tag{8.8}$$

$$\frac{W_4}{W_3} = 0.988577$$

According to Raymer, the descent for landing is estimated to be between 0.99 and 0.995. For this mission, the estimate was 0.99.

$$\frac{W_5}{W_4} = 0.99$$

Since the mission specifies a return trip directly after unloading, the same estimation of weight fraction from the descent for landing was used to estimate the landing and taxi back. The taxi back was not taken into account, however, because it was already considered in the second takeoff.

$$\frac{W_6}{W_5} = 0.993$$

Next, the second takeoff was estimated using the same Raymer estimation as before.

$$\frac{W_7}{W_6} = 0.99$$

The climb and acceleration estimation was calculated using the same equation as in the first climb.

$$\frac{W_8}{W_7} = 1.0065 - 0.0325M$$

$$\frac{W_8}{W_7} = 1.0065 - 0.0325(0.8)$$

$$\frac{W_8}{W_7} = 0.9805$$

The third cruise is only at 20000 ft but still at $M = 0.8$.

$$\frac{W_9}{W_8} = e^{\frac{-RC}{V(L/D)}} \tag{8.9}$$

$$\frac{W_9}{W_8} = e^{\frac{-600nm0.6/hr}{0.8(589.5kts)(13.2)}} \tag{8.10}$$

$$\frac{W_9}{W_8} = 0.949614$$

The second descent for landing was going to be 0.99 because the descent is from 20000 ft instead of 1000 ft as it was for the outbound mission.

$$\frac{W_{10}}{W_9} = 0.99$$

For the second time, the taxi back actually had to be included in the final weight fraction estimate.

$$\frac{W_{11}}{W_{10}} = 0.992$$

The final weight over the initial weight was calculated by multiplying each weight fraction. The end result of this calculation was then used to calculate the weight of the fuel, which was put into the total weight equation to yield the first iterative calculation of weight.

$$\frac{W_{11}}{W_o} = 0.728598$$

$$W_{fuel} = 1.06(1 - \frac{W_{11}}{W_o})W_o$$

$$W_{fuel} = 1.06(1 - 0.728598)200000lb \tag{8.11}$$

$$W_{fuel} = 57537.3lb$$

Now the total weight was calculated from all of the above information.

$$W_o = W_{\text{crew}} + W_{\text{fixed payload}} + W_{\text{dropped payload}} + W_{\text{fuel}} + W_{\text{empty}} \tag{8.12}$$

$$W_o = 600lb + 60000lb + 57537.3lb + 0.46048(200000lb)$$

$$W_o = 210547lb$$

After only one iteration, this was a very reasonable takeoff gross weight calculation. The method calls for iterations until the initial guess and the final calculation are within a few percent of each other. This calculation is almost exactly 5% larger than the initial guess, and the Mason Project was happy with this weight. 210000 lbs was not unreasonable for an aircraft of this size. The fuel weight was an initial concern because it might not be enough fuel for the design mission; however it was not a concern for the transoceanic ferry mission due to the allowance for aerial refueling.

9. Mission Analysis

9.1. Takeoff Analysis

An important aspect in the analysis of an aircraft's performance is how the plane performs at takeoff. To be able to perform the full takeoff analysis, a program needed to be written which could complete the needed calculations. The basis of such a program was already written by Sean Lynn and provided for the use of the Mason Project on the software website of Dr. Mason. The original program was written in FORTRAN and was later converted to C. The program provided a good foundation for the takeoff program as it is currently, but also lacked some of the considerations, like wind, that the current program contains. Going from the original takeoff program, a new program was written which was of more use. The original program was converted into MATLAB and modified with a new ODE solver which performed the required calculations. The code was modified several times and considerations for vectored thrust, wind, and a new thrust equation were added.

The finished MATLAB takeoff program made takeoff analysis considerably easier. The first step in using the program was to calculate the thrust coefficients for the aircraft. It is important to understand how the thrust varies with the velocity of the plane because it will change as the plane is accelerating down the runway. Looking through the engine deck the ways in which the velocity affected the thrust on the engines could be determined. The takeoff program calculated the equation of a spline through the different thrusts. Those coefficients were input into the aircraft configuration file which contains some aircraft specific information to be passed into the takeoff program. The following step to running the takeoff program was to determine the density for the takeoff conditions. The RFP required the plane be able to take off on a hot day, at 95˚F. The density calculation function calculated the sea level density on a hot day to be 0.00222265 sl/ft^3. The next step was to ensure that all the aircraft's configuration characteristics were in the aircraftconfig.m file of the MATLAB program. The acceleration due to gravity, the weight of 210,547 lbs, planform area of 2280 ft^2, the C_{Lmax} of 4.96 and other drag and lift coefficients for the air and the ground were input into the configuration file. Other factors that went into the configuration file were the friction coefficients of the ground and the braking coefficients. A consideration for vectored thrust was left at 0˚ because the upper surface blowing characteristics were incorporated into the $C_{Lmax.}$ The stall margin was put in to be 1.2; the decision time for an

engine out scenario was 3 seconds. The test case was run for a wind speed of 0 ft/s although that could be altered to the user's input. The amount of engines was inserted to be 4 so that the program could know how to calculate one engine out characteristics specific to the S.T.O.R.K.

After running the takeoff program, a great deal of useful information was gathered. Initially, the most important number to look at was the balanced field length to ensure that it fit under the RFP requirements. The balanced field length for the S.T.O.R.K. was found to be 2114 ft. That is well below the required 2500 ft found in the RFP. This result provided mixed reactions. Since there was a lot of room to be able to change the configuration of the aircraft, it was not in trouble of failing to meet one of the requirements if it extended the balanced field length. However, one of the problems with such a low balanced field length was that the design more than likely had excessive thrust or some features which it did not need. The Mason Project believed that extra thrust would be needed to achieve the Mach 0.8 requirement, and that it was also a safer alternative with the one engine out upper surface blowing control effects. Under normal circumstances, the aircraft will takeoff at 204 ft/s and will use 1649 ft of runway. The ground run time is just under 16 seconds so the aircraft can get off the ground fairly quickly. The full printout provided in Table 9.1 below gives a summary of the takeoff.

Table 9.1 Takeoff Analysis Summary

<<<<<<<<<<<<<<<<Normal Takeoff Summary>>>>>>>>>>>>>>>>

Rotation Air Velocity	=	167.62682	(ft/s)
Rotation Ground Velocity	=	167.62682	(ft/s)
Liftoff Air Velocity	=	205.75705	(ft/s)
Liftoff Ground Velocity	=	205.75705	(ft/s)
Ground Velocity over obst.	=	210.76262	(ft/s)
Air Velocity over obst.	=	210.76262	(ft/s)
Rotation Distance	=	957.55924	(ft)
Liftoff Distance	=	1518.34297	(ft)
Distance to obst.	=	1914.50340	(ft)
Rotation Time	=	10.91226	(sec)
Liftoff Time	=	13.91226	(sec)
Time to obst.	=	15.82624	(sec)
TOTAL TAKEOFF DIST	=	1914.50340	(ft)
TOTAL TAKEOFF TIME	=	15.82624	(sec)

<<<<<<<<<<<<<<<< OEI Takeoff Summary >>>>>>>>>>>>>>>>

Critical Velocity	=	122.5668	(ft/s)
Decision Velocity	=	153.1964	(ft/s)
Velocity over obst.	=	196.2572	(ft/s)
Critical Distance	=	484.3736	(ft)
Decision Distance	=	898.0185	(ft)
Balanced Field Length	=	2113.7609	(ft)
Critical Time	=	7.6579	(s)
Decision Time	=	10.6579	(s)
OEI Takeoff Time	=	17.3551	(s)

9.2. Landing Analysis

In addition to requiring certain conditions be met for takeoff, the RFP also had certain qualifications for landing. It required the airplane be able to clear a 50 ft obstacle and land on a useful runway length of 3000 feet. The plane also needs to be able to land in a crosswind of up to 25 knots and a tailwind of 5 knots. Much like the takeoff program, a new program was written to analyze the landing characteristics of this aircraft. The program required several characteristics of the aircraft's configuration as well as the landing environment. It was assumed that some fuel was either burned off during flight or can be dumped if needed for a tricky landing, and therefore a weight of only 180,000 lbs was used for the landing calculations. The aircraft's powered lift system required some thrust on landing to achieve the high level of lift required in the mission's STOL capabilities. The landing was evaluated at 25,000 lbs of thrust. The obstacle height and other landing parameters such as the density and different drag and lift coefficients were input into the program. The considerations for the time delay before braking, and for wind were also entered into the program. With all the factors accounted for, the program could be run which followed Daniel Raymer's method for calculating landing parameters. The results were good and show that the S.T.O.R.K. has little trouble landing in the allowed space. The plane should touch down at 142 ft/s. After approaching for approximately 800 ft, the aircraft will flare, touchdown and taxi for 220 ft and then the brakes would be applied for another 1150 ft. The total landing distance for this aircraft is 2175 ft. Upon realizing that the plane would be able to land according to the requirements, it was decided that the implementation of reverse thrusters was not necessary. There was no need to burden the aircraft with extra cost, weight and complicated machinery that comes along with the reverse thrusters. A more detailed printout of the landing results is provided in Table 9.2 below.

Table 9.2 Landing Analysis Summary

```
============== Landing Results ======================
=====================================================
  Stall Velocity                 =   129.1727  ft/s
  Approach Velocity              =   155.0072  ft/s
  Touchdown Velocity             =   142.0900  ft/s
  Average Flare Velocity         =   148.5486  ft/s
  Vertical Touch Down Velocity   =     8.4190  ft/s
  Horizontal Touch Down Velocity =   141.8403  ft/s
  Approach Angle                 =     3.3968  deg
  Flare Height                   =     2.4080  ft
  Approach Distance              =   801.8121  ft
  Flare Distance                 =    81.2099  ft
  Free Roll Distance             =   142.0900  ft
  Braking Distance               =  1149.1202  ft
  Total Landing Distance         =  2174.2322  ft
```

9.3. Mission Analysis

An important aspect of measuring the S.T.O.R.K.'s capabilities was to examine how well it performed in the two missions stated in the RFP. The aircraft was designed primarily to fulfill the Ferry Mission of the RFP. The main concerns for accomplishing this mission was being able to takeoff and having enough fuel to complete the range portion of the mission. A program provided to the team was used to do a complete analysis of the mission performance. Several key setup files needed to first be completed before the missions could be evaluated. A file containing the aircraft's configuration was created which possessed a great deal of information about the aerodynamic qualities of the S.T.O.R.K. as well as other factors such as the size of the fuel tanks. Another file was created containing the detailed thrust values for this aircraft. This file had the information to tell the program how much thrust and how much fuel each engine would be using. The other important information that was put into the program was the mission files. Two files were created, one for the design mission, and one for the ferry mission. After loading all the files to the program, a detailed analysis of the S.T.O.R.K.'s mission performance could be evaluated. Information such as range, lift to drag ratio, time, fuel use and speed were calculated.

For the design mission described in the RFP, a mission file was created and used in the performance program. The results were very favorable. With the fuel tanks holding 60,000 lbs of fuel, there was some concern that the aircraft could not meet the requirements without needing to

refuel. In the end, the S.T.O.R.K. was found to perform this mission using just over 55,000 lbs of fuel. The entire time of the mission is just under 200 minutes and covers a total range of 1,200 nautical miles. More details on each segment of this mission are provided below in Table 9.3.

Table 9.3 Mission performance summary for design mission

Design Mission						
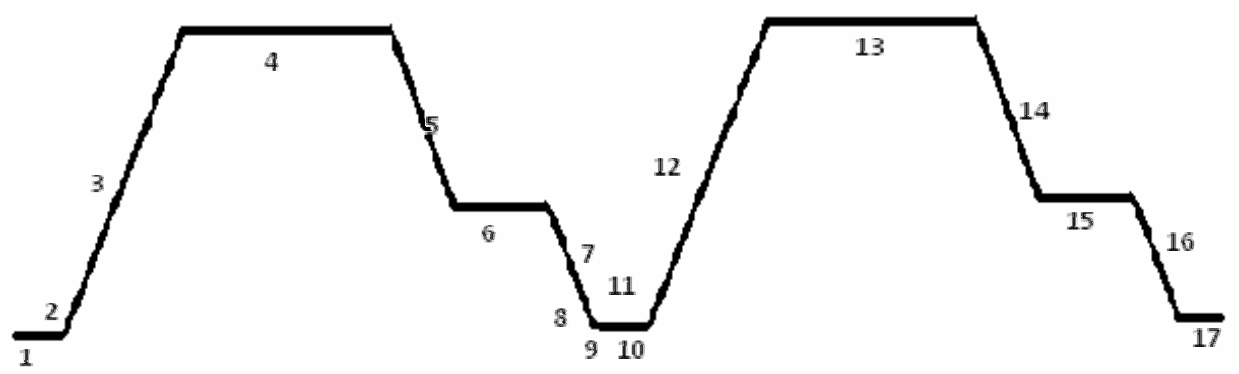						
PAYLOAD = 60,000 LB		TOGW = 210,547 LB INTERNAL FUEL = 60,000LB				
TAKEOFF DIST = 1713 FT BFL = 1893 FT TAKEOFF TIME = 14.36 SEC		LANDING DIST = 2174 FT				
MISSION SEGMENT	MACH	ALT (FT)	L/D	TIME (MIN)	FUEL (LB)	DIST (N MI)
1. WARM-UP, TAXI	-	SL	-	8	1332	-
2. TAKEOFF	0.18	SL	-	2	1788	-
3. CLIMB TO CRUISE ALT	0.55	22,000	-	21	6714	119
4. CRUISE AT BCA M = 0.8 FOR 500 NM	0.8	35,000	12	50	11134	381
5. DESCEND TO 1000 FT	0.8	1000	-	-	-	-
6. CRUISE M = 0.6 FOR 100 NM	0.6	1000	6.7	15	6344	100
7. 3/4 THRUST FOR 5 MIN	0.6	1000	-	5	3501	-
8. LANDING	0.12	SL	-	-	-	-
9. DEPLOY FDAV	-	-	-	-	-	-
10. WARM-UP, TAXI	-	SL	-	8	2041	-
11. TAKEOFF	0.18	SL	-	2	1642	-
12. CLIMB TO CRUISE ALT	0.51	20,000	-	8.9	3256	47
13. CRUISE AT BCA M = 0.8 FOR 500 NM	0.8	35,000	9.2	59	11698	453
14. DESCEND TO 1000 FT	0.8	1000	-	-	-	-
15. CRUISE M = 0.6 FOR 100 NM	0.6	1000	4.6	15	6178	100
16. 3/4 THRUST FOR 5 MIN	0.6	1000	-	5	3501	-
17. LANDING	0.12	SL	-	-	-	-
TOTALS	-	-	-	197	55,351	1200

After satisfaction was achieved in designing for the design mission, analyzing the ferry mission was the next task performed. Due to the longer distance in cruise for this segment of the mission, an aerial refueling is required. The mission calls for 3,000 nautical miles of cruise, and the S.T.O.R.K. would normally run out of fuel after 2,000 nautical miles. At that point, the aircraft slows for a short distance and is refueled. The total amount of fuel required in this mission, according to the performance program, is 100,100 lbs with reserve fuel considerations. A full load of fuel is not needed at refuel, only approximately 40,000 lbs. The total mission time including the reserve fuel considerations is 395 minutes. More details on each segment of this mission are provided below in Table 9.4.

Table 9.4 Mission performance summary for ferry mission

Transoceanic Ferry Mission

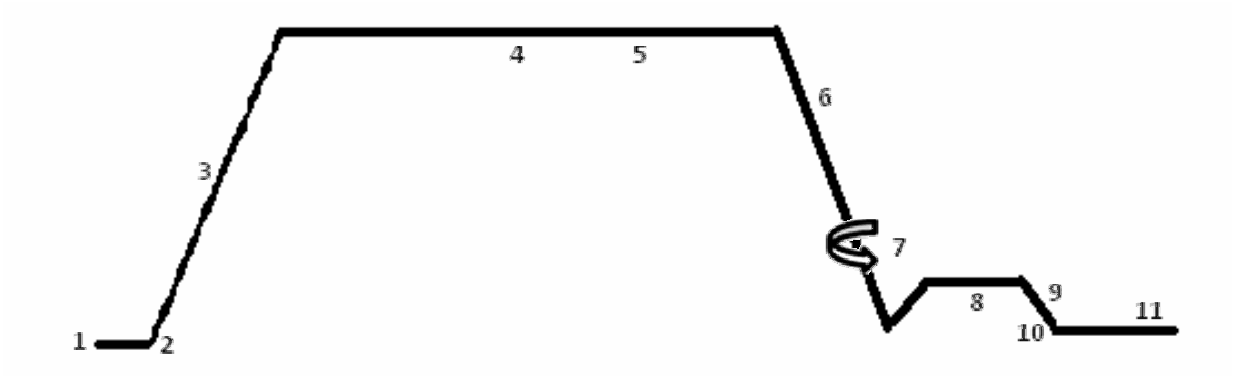

PAYLOAD = 60,000 LB		TOGW = 170,547 LB INTERNAL FUEL = 60,000LB				
TAKEOFF DIST = 1914 FT BFL = 2113 FT TAKEOFF TIME = 15.85 SEC		LANDING DIST = 2174 FT				
MISSION SEGMENT	MACH	ALT (FT)	L/D	TIME (MIN)	FUEL (LB)	DIST (N MI)
1. WARM-UP, TAXI	-	SL	-	8	1332	-
2. TAKEOFF	0.18	SL	-	2	1788	-
3. CLIMB TO CRUISE ALT	0.54	22,000	-	13	4672	74
4. CRUISE AT M = 0.8 FOR 3200 NM	0.8	35,000	11.4	280	75,734	3,126
5. REFUEL AFTER 2000 NM	0.4	35,000	12.6	11	1,222	50
6. DESCEND TO 5000 FT	-	5,000	-	-	-	-
7. RESERVE FUEL: 45 MIN LOITER	0.23	5,000	13.1	45	5,786	0
8. RESERVE FUEL: 150 NM DIVERSION	0.32	5,000	11.4	32	8,003	150
9. DESCEND TO SL	-	SL	-	-	-	-
10. 3/4 THRUST FOR 5 MIN	-	SL	-	5	1,788	-
11. TAXI AND PARK	-	SL	-	10	1,652	-
TOTALS	-	-	-	395	100,755	3,350

10. Structures

10.1. Strut Braced Wing Concept

The design approach taken which included the use of struts provides a unique structural design. The main advantage of the use of the struts was the reduction in the critical loads for which the wing must be designed. Maximum positive loads no longer need to be the maneuvering load that the wing structure is designed to accommodate. The struts are not effective under negative loading, but rather only under a specific positive load, which helps reduce the loading on the wing without a major weight penalty from designing a strut that does not buckle under negative loads. In addition to this, the wing geometry can be changed such as: increasing the aspect ratio, decreasing wing t/c ratio, and reducing sweep. Figure 10.1 below shows the strut design.

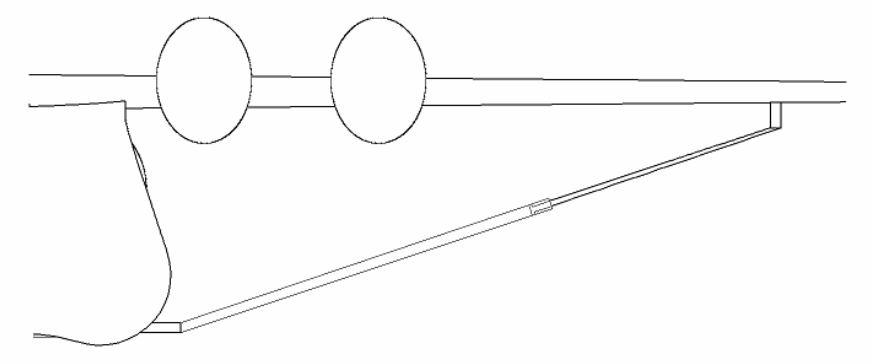

a)

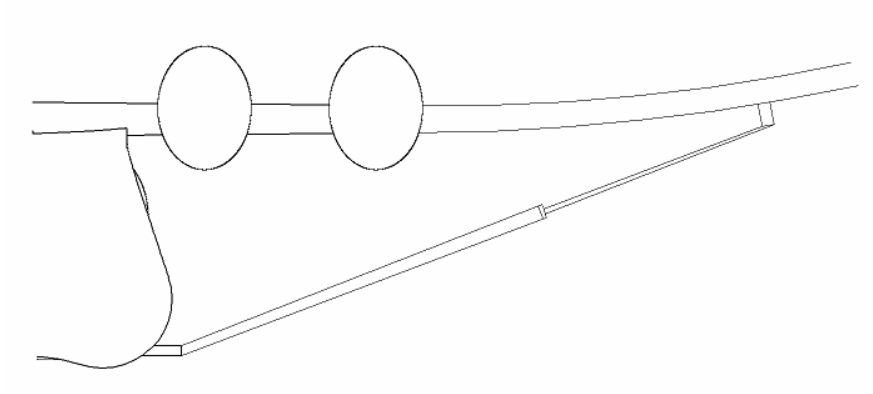

b)

Figure 10.1 Wing with Telescoping Sleeve Strut a) Wing with Strut Inactive with Slack Distance b) Wing with Strut Active

Below is the V-n diagram, Figure 10.2, to show the flight envelope as well as the experienced loads. The shear and bending moment diagrams below, Figures 10.3 and 10.4, show the forces experienced by the wing. The plot for the shear force and moment diagrams makes the benefit of the strut very clear. There is a significant decrease in shear forces and bending moments inboard of the strut.[4] From these bending moments, the required material thicknesses required for both the skin and stringer/spars was determined.

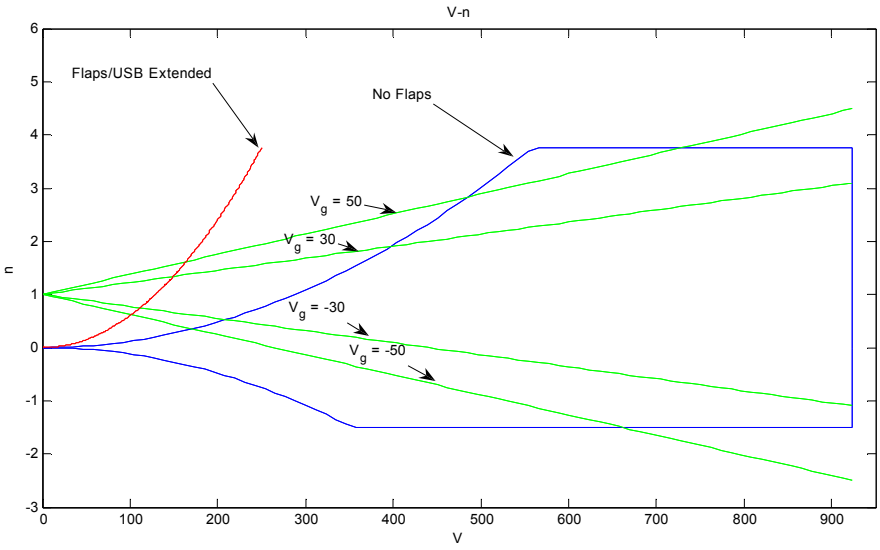

Figure 10.2 V-n Diagram

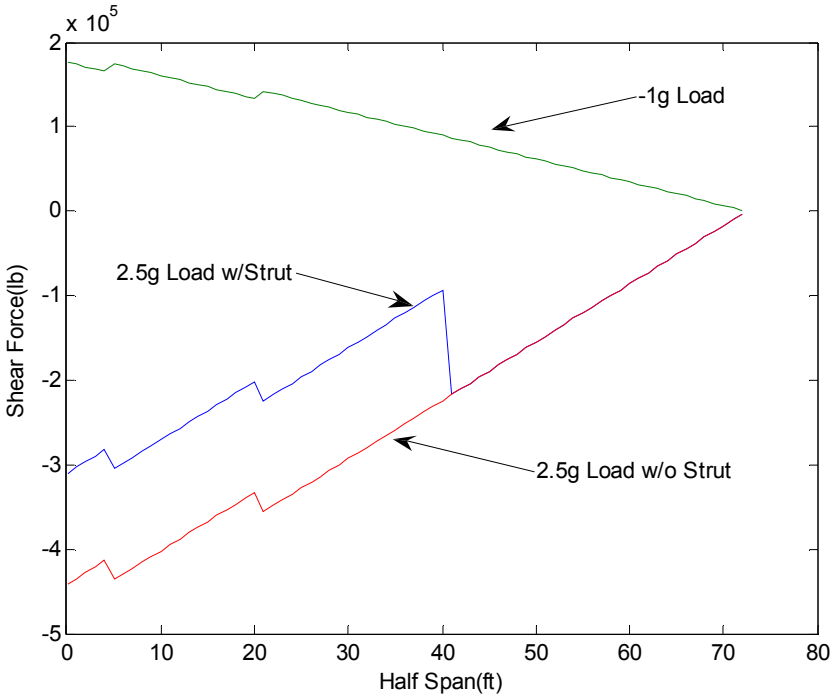

Figure 10.3 Shear Force Diagram

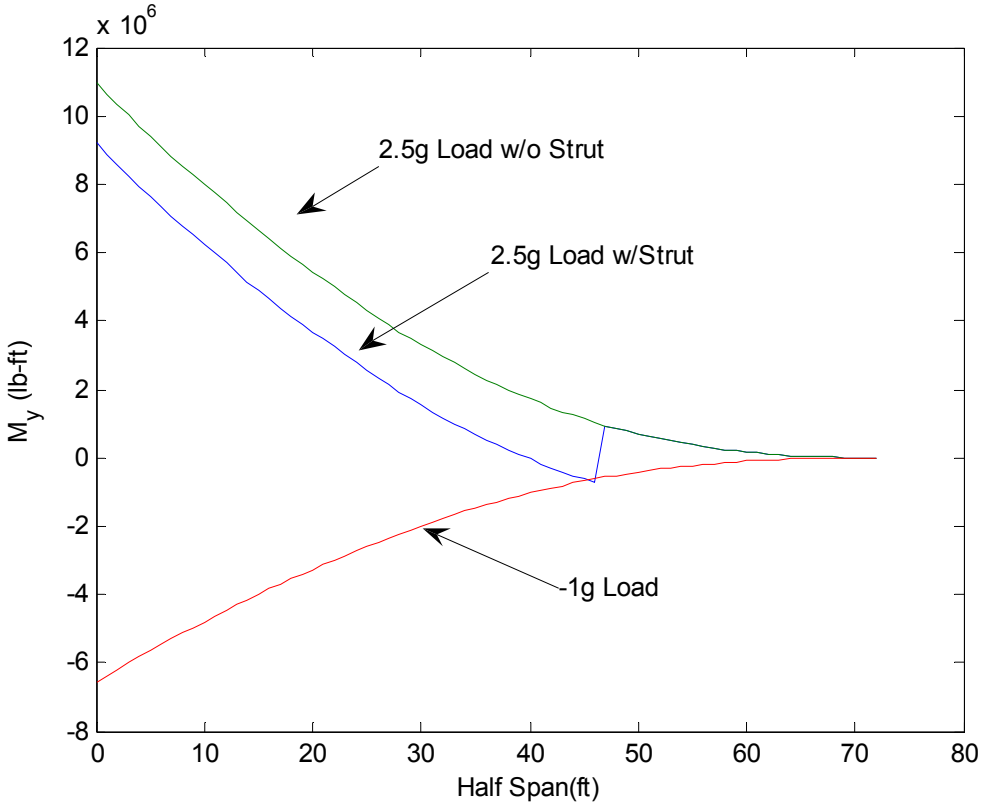

Figure 10.4 Bending Moment Diagram

10.2. Structure

Another benefit of the strut was that with reduced loading, the wing did not need a complicated and heavy structure. With the increased use of composites to lower the weight, the more simplistic components would be easier to produce. The wing, horizontal tail, and vertical tail would all be composed of twin spar structures with integrally stiffened skin panels. The wing can be seen in Figures 10.5 and 10.6, and the tail structure can be seen in Figure 10.7. Integrally stiffened panels are a way to take advantage of the use of composites. They are single structures that are composed of a thin skin with stringer-like stiffened sections such as Figure 10.8 below. The number and spacing would be determined by an optimization code, which would also determine the thickness of the stiffeners and spars. This was done from using the loads determined in the loading diagrams and an idealized wing box structure. The idealized wing box consists of a single cell two spar rectangular box.

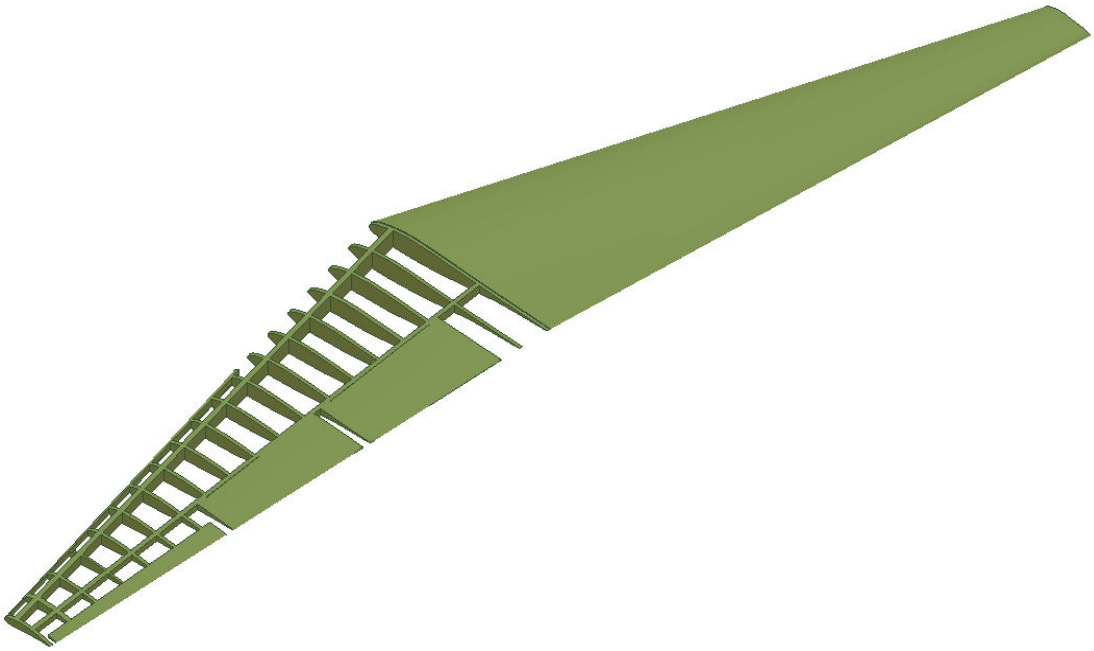

Figure 10.5 3-D Wing Structure

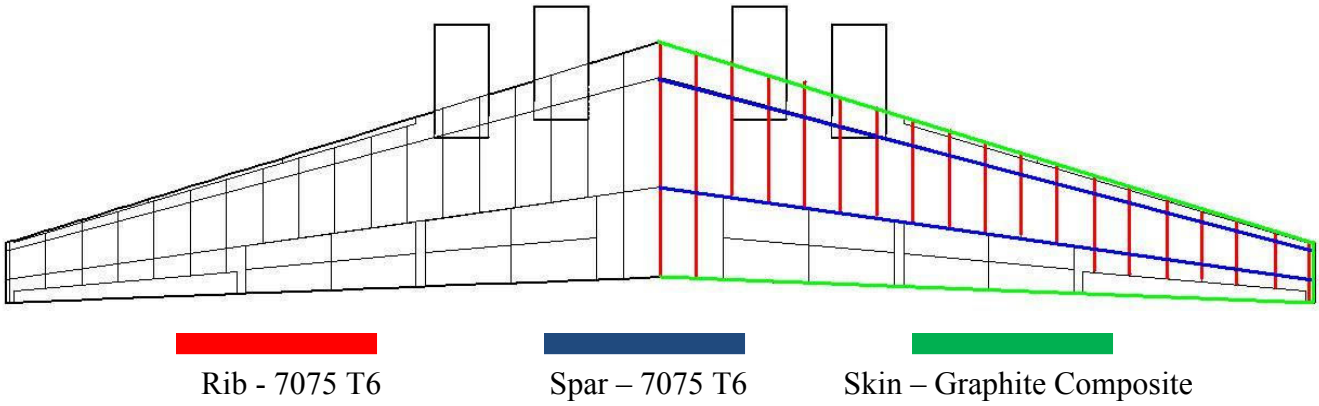

Figure 10.6 Wing Structure

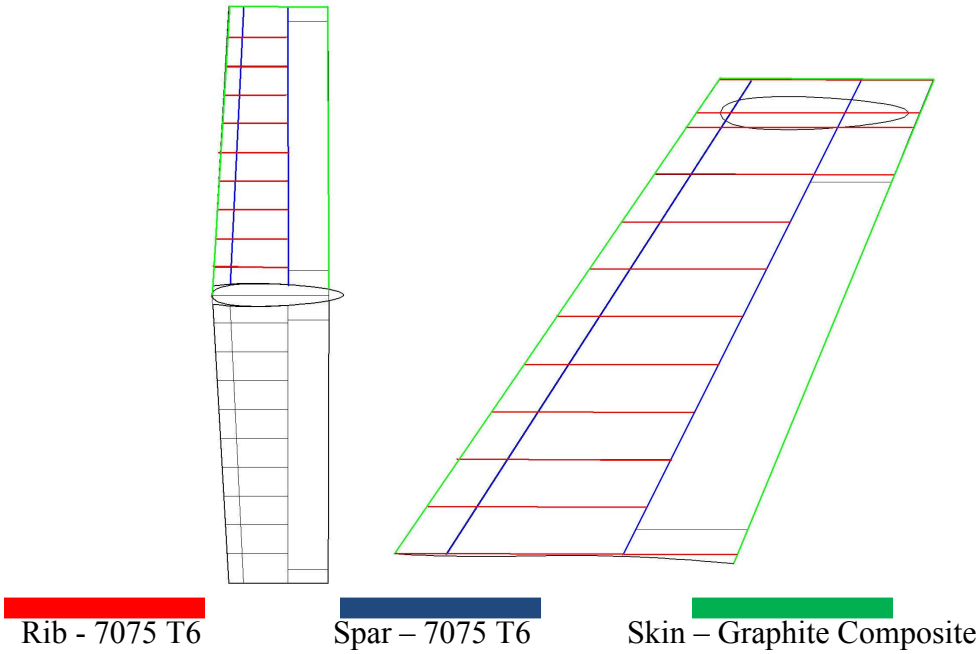

Figure 10.7 Tail Structure

Figure 10.8 Example of Integrally Stiffened Panel

This use of the strut braced wing made it possible to take the span of the wing from 104ft to 145ft. This is a significant increase in span allowing the reduction in drag without a great weight

penalty. While the span of the wing could have been pushed farther, it was decided to reduce the weight in the wing and strut structures. This becomes more important when taking into account the use of the USB system which increases the weight of the wing.

From the bending moment diagram, the required thickness for the stiffeners can be determined. To make the measurements easier, the wing box was assumed to be a symmetrical, single cell structure. By making these assumptions the equation for the required thickness of the stiffeners and spars can be determined from equation 10.1. This thickness distribution can be seen in Figure 10.9, and the overall thickness will taper according to equation 10.2. In addition to this, the thickness for the aluminum spar booms will taper as shown in Figure 10.10, and the stiffeners will taper as shown in Figure 10.11.

$$A_y = M_y / (\sigma_u \bullet t) \qquad (10.1)^5$$

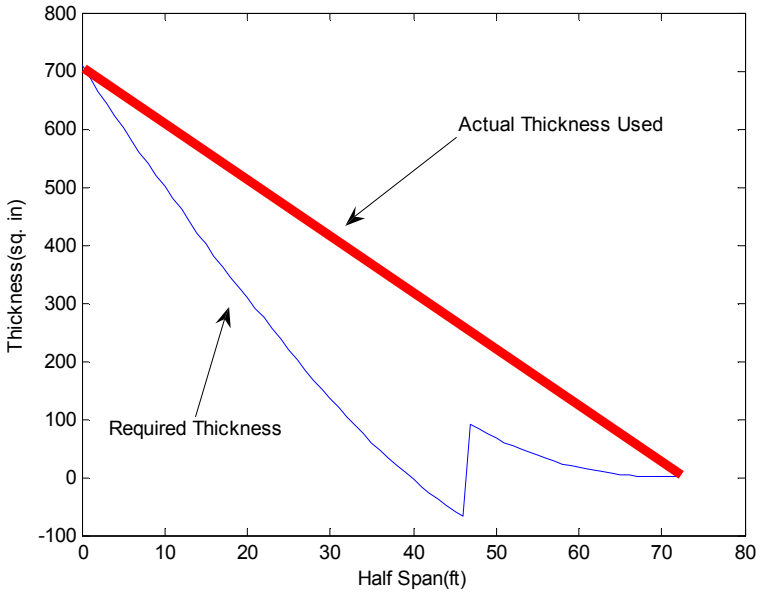

Figure 10.9 Thickness Distribution

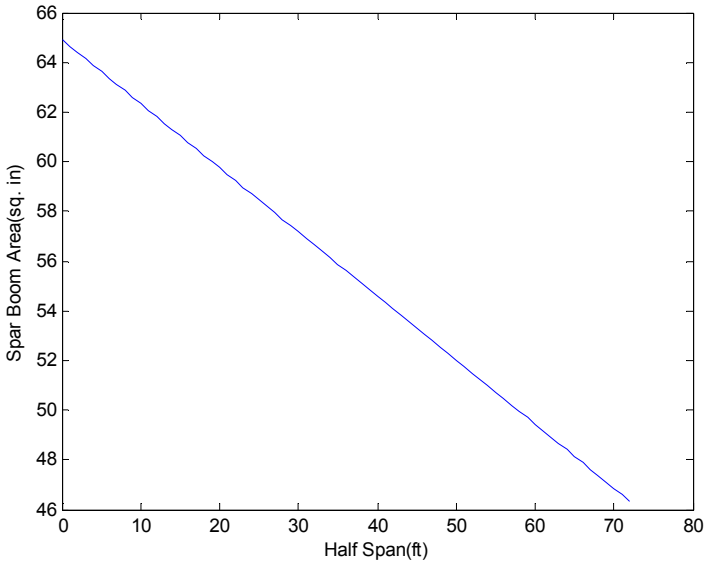

Figure 10.10 Spar boom area taper

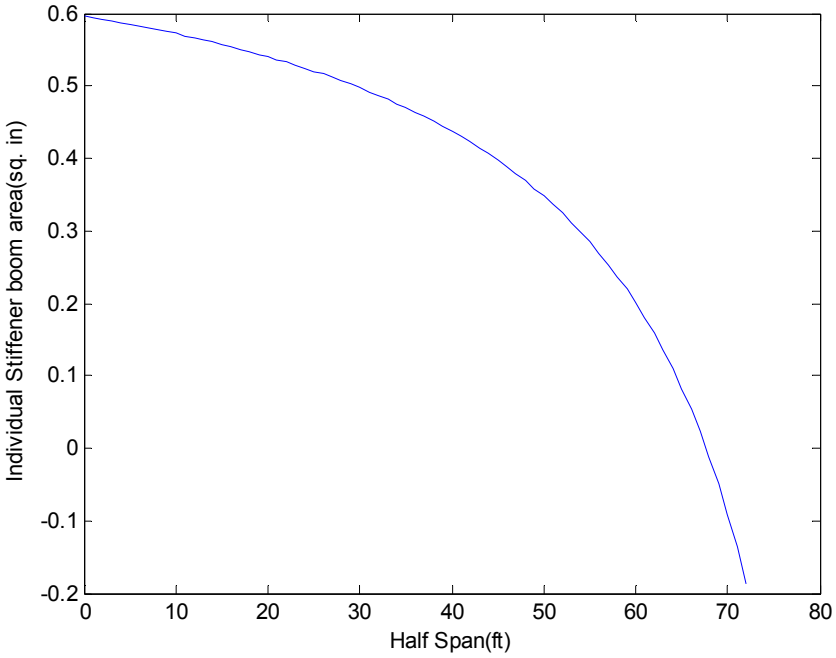

Figure 10.11 Stiffener boom area taper

As can be seen in Figure 10.9, the actual required overall thickness is much less than that of the thickness used. This is due to the fact that it would be difficult to produce a spar that was tapered as was required. Therefore it is tapered linearly as shown in Figure 10.9. From there, the

taper of the spar booms was determined and shown in Figure 10.10. With that finalized, the thickness distribution for the stiffeners can be determined. Using stiffeners spaced every other inch, the required thickness is shown in Figure 10.11. For the section of the wing where the stiffener boom area is negative, on Figure 10.11, there is no need for the stiffeners to extend any farther as it is the location along the spar which carries all of the bending moment.

A serious side effect of the use of powered lift system is the increase in undisturbed air behind the wing and engines. This would result in the use of large control surfaces on a traditional tail and for this reason, a high T-tail was employed. This use of the T-tail, however, provided certain structural difficulties. The vertical tail structure needed to become larger to support the horizontal tail, and the horizontal tail needed be stiffened to withstand flutter. This increase in required T-tail stiffness can be seen in Figure 10.12 below.

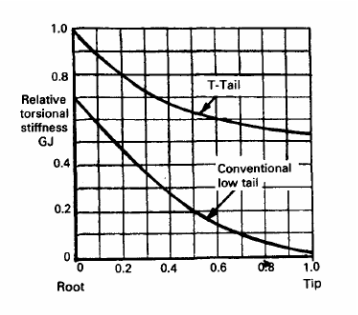

Figure 10.12 Required T-Tail Stiffness

The next major component of the structure was the strut. The idea behind the strut was to have it engage at a point so the load on the wing under positive loading is the same as negative loading. Therefore it seemed reasonable that it should engage at a load of 1g. This, however, would result in the strut loading and unloading frequently, and therefore it was designed to engage at a loading of 1.2g to avoid fatigue of the strut. The design of the strut can be seen in Figure 10.12. It was decided to use a strut made of the same 7075 T-6 Aluminum as the spars. The cross section of the aluminum was decided to be 7.5in^2, which resulted in an allowable strut force of 36,000lbs. With the angle between the strut and the strut offset member of 145°, the result is a vertical strut force of 25,000lbs and a horizontal strut force of 11,000lbs. The strut was designed to attach to the fuselage at the same fuselage frame as the landing gear, to only need to bolster the strength of a single fuselage frame.

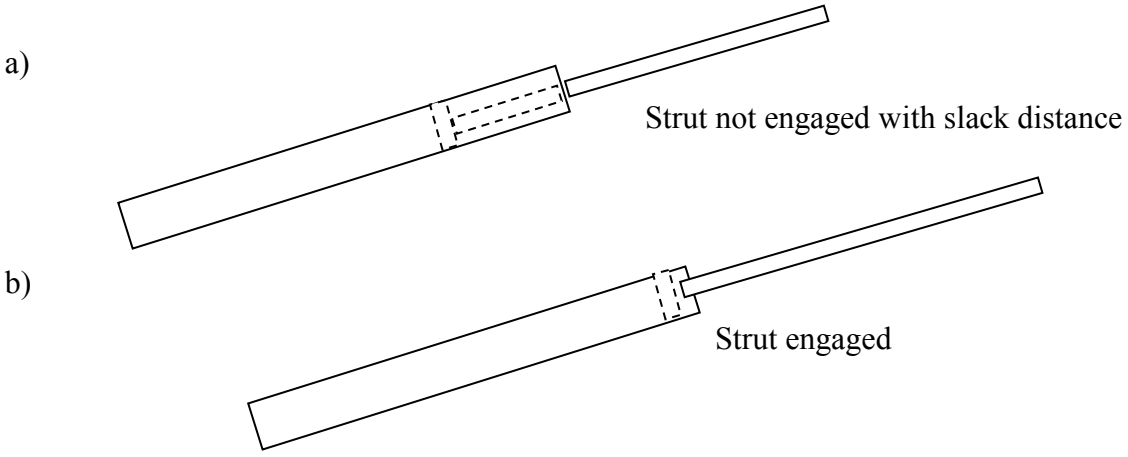

Figure 10.12 A) Strut Under No Load with Slack Distance b) Strut Engaged

10.3. Materials

One aspect that can greatly reduce the weight of the airframe is the selection of materials, mainly the use of composites. For heavily loaded and complex structures of the aircraft, it was decided to use 7075 aluminum due to its strength and weight, as well as the ability to produce complex structures more easily[6]. Therefore within the wing, horizontal tail, and vertical tail the spars and ribs will be constructed of aluminum. The frames for the fuselage will also be produced from aluminum.

In addition to the use of aluminum, composites were be heavily relied upon for the structure of the airframe. The aim of the design was to use approximately 30% composites by weight. The use of composites can result in roughly a 25% weight reduction over replaced components. This would result in lowering the weight of the aircraft by 7.5% over a non-composite constructed aircraft[7]. While modern manufacturing finds the use of composites much easier, there is still an associated increase in cost with the use and production of composites. For this reason it was felt that to best way to reduce weight without a drastic increases in cost would be to produce simple components out of composites, such as skins and stringers. One of the benefits that the composites give is the ability to produce single large skin panels. This means that skin splicing

that is usually done with aluminum skins can be avoided and further help reduce weight. The composite used is a high strength graphite epoxy matrix which meets the stress requirements to which the skin and stringers will be exposed.

Table 10.1 Materials Strengths[4]

Material	Density(lb/in^3)	Yield Stress(psi)
7075-T6 Al	.101	72000
High Strength Graphite Epoxy	.056	46000

The downside with the use of composites is the cost. If you look at the cost of Aluminum 2024 and the graphite epoxy composite that is used to replace it, the composite is quadruple the cost of the equivalent-strength aluminum.[7] This is offset by the reduction in weight of approximately 40%. The cost of the use of hand-layup versus tape lay-up manufacturing as well as pre-preg versus woven cloth construction needed to be weighed versus the increase in man hours required for the different construction methods.

10.4. Landing Gear

The RFP stated that the landing strip has a CBR of 4-6 (comparable to a blacktop surface), which presented some challenges to configuring the landing gear. A dual-tandem tricycle system was therefore selected for the landing gear as it provided the most stability and durability. This decision was also based on two other important factors: space and weight. There is a limited amount of space under the fuselage for wheels and struts, and an increase in wheels meant an increase in weight. The current landing gear configuration optimizes space and weight to create an efficient system for this aircraft.

The original landing gear design called for two nose wheels, and eight aft wheels (four on each strut) for a total of ten wheels. However, with the factor of safety included, ten reasonably sized wheels were not enough to hold the weight of the aircraft. The final design has one single nose strut with two wheels, and twin struts in the rear with six wheels on each strut, a total of 14 wheels. The two front wheels are set side by side, and the rear wheels are three rows of two wheels each, also set side by side. The rear configuration was chosen due to the decrease in drag compared to the wider initial design. A conventional rear configuration of two rows with three

wheels across (such as in the Boeing C-17) was considered, however, the unnecessary drag penalty was avoided by using three rows of two across. All calculations were made using equations from Raymer; a 7% margin was added along with the FAR 25 requirement of 25% increase in load calculations (factor of safety). Equations and calculations are shown below.

$$TOGW = 210547 lbs$$
$$(1 + 0.25 + 0.07) * 210547 lbs = 277922 lbs$$
$$277922 lbs * 0.10 = 27792.2 lbs$$
$$27792.2 lbs / 2 = 13896.1 lbs$$
$$277922 lbs * 0.90 = 250130 lbs$$
$$250130 lbs / 12 = 20844.2 lbs$$

According to the above calculations, each front tire must be hold 13986.1 lbs, and each rear tire must hold 20844.2 lbs.

With the weight information for each tire, Raymer's book was used to determine each tire sizing and type. The 37" x 14.0" tired was found to be the best fit for this design. This tire is designed for speeds well within this design's flight envelope (specifically takeoff and landing). The design speed for the tire is 225 mph and the maximum load for each tire is 25000 lbs. The maximum width of each tire is 14.0" with a rolling radius of 15.1 in, a wheel diameter of 14.0" and 24 plies. Also, for a CBR of 4-6, each tire pressure is 160 pounds per square inch.

11. Stability and Control

In the process of designing a transport aircraft that would meet the needs of both the mission and the military, it was necessary to have a full understanding of what the aircraft would need to perform the mission to the best of its ability, as well as what reactions it will have when in flight. To create an aircraft that will out-perform the competition, a study of the stability of the aircraft was necessary. In the following section there is an analysis of the overall stability of the S.T.O.R.K. as well as estimations to the control surface sizing necessary to fly and control the aircraft to its maximum potential.

11.1. Longitudinal Static Stability

To create a stable aircraft it was necessary to approximate a fairly large static margin. The larger the static margin, the less "touchy" the aircraft will be to the pilots' controls and also the less elevator authority would be needed. There is, however, the possibility for too much static margin, which would easily lead to an elevator stall on the aircraft. For this reason, a desired static margin of 13% was the goal for the design. This goal was decided upon through the understanding that having the neutral point and the center of gravity point set to a specific distance from each other would allow for both the aircraft to handle like a traditional transport, as well as give the pilot some ease in controlling the aircraft if the pilot were to need maneuverability during flight. With a static margin goal set, the neutral point was calculated through a method provided by Simons[7]. To solve for the neutral point the following equation was used.

$$h_n = h_o + \eta_s V_s \left(\frac{a_s}{a_w}\right)\left(1 - \left(\frac{d\varepsilon}{d\alpha}\right)\right) \tag{11.1}$$

Where

$$V_s = \frac{S_s L_s}{S_w c} \tag{11.2}$$

Using Equation 11.1 a neutral point of approximately .388 was found. This would equate to a neutral point that rested approximately 38.8% *MAC* of the wing. With the neutral point

determined and a desired static margin of 13% *MAC,* the center of gravity was calculated to fall at approximately 25.8% *MAC* on the wing. Over the course of the aircrafts' mission, there will be a center of gravity shift; however that shift is expected to be small. This shift is due to the fact that though there will be a fuselage fuel tank, it has been designed to be located directly below the aircrafts' center of gravity. The fuel tanks that are located in the wings would have very little effect on the longitudinal center of gravity of the aircraft[8]. The other stability point which was needed for calculations was the aerodynamic center. This was calculated using the following equations provided by Raymer[9].

$$x_{ac} = x_{c/4} + \Delta x_{ac}\sqrt{S_{wing}} \tag{11.3}$$

Where

$$\Delta x_{ac} = .26(M - .4)^{2.5} \quad \text{(for .4<M<1.1)} \tag{11.4}$$

Using equations 11.3 and 11.4 an aerodynamic center of 7.98 ft from the leading edge of the wing was found. This places the aerodynamic center around 27.5% *MAC* and at a distance of 36.78 ft from the nose of the aircraft. It should be noted that the center of gravity is located forward of the aerodynamic center. A configuration such as this will result in a stable aircraft.

On each of the three axes about which the plane maneuvers, there will be individual set stabilities. The three axes are longitudinal, lateral and directional. These three axes all cross in the common location of the center of gravity. These axes will change as a result of the changing center of gravity throughout the aircraft's flight. Longitudinal stability is the stability of the pitching forces of the aircraft. The pitch of the aircraft is the up and down movement of the nose. A pitch up moment allows for climb, however it could result in stall if the pitching moment is not compensated for by the control surfaces on the tail. When it comes to longitudinal stability, it is desired to have the aircraft return to its stable state with as little pilot input as possible. To obtain this reaction, it would be necessary to have positive stability on the pitching moment arm. This desired outcome would allow for the pilot to have minimal interaction with control units in the cockpit and still have the unstable nose up moment return to the stable nose down state. This return to a stable position comes about after going through a slow phugoid oscillation. This slow oscillation allows for the pilot to have control of the aircraft without needing his strength to maintain the maneuverability of the aircraft. Having the least amount of pilot interaction creates

an aircraft that responds better and more efficiently to non stable states into which the aircraft may fall. To calculate the aircraft's pitching moment, equations provided by Etkin and Reid[10] were used. These equations are as follows:

$$C_m = C_{m_{ac_{wb}}} + C_L(h - h_{n_{wb}}) + -\overline{V}_H C_{L_t} + C_{m_p} \tag{11.5}$$

Where

$$C_{m_{ac_{wb}}} = \frac{2}{S\overline{c}}\int_0^{b/2} C_{l_b} xcdy + \frac{2}{S\overline{c}}\int_0^{b/2} C_{m_{ac}} c^2 dy \tag{11.6}$$

$$(h - h_{n_{wb}}) \cong -K_n \tag{11.7}$$

$$\overline{V}_H = \frac{\bar{l}_t S_t}{\bar{c} S} \tag{11.8}$$

$$C_{L_t} = \frac{L_t}{\frac{1}{2}\rho V^2 S_t} \tag{11.9}$$

$$C_{m_p} = \frac{T}{W} C_L \frac{z_p}{\bar{c}} \tag{11.10}$$

Using Equations 11.5 through 11.10 a pitching moment of -1.23 was found. When this pitching moment is compared to the estimated pitching moments of traditional jet transports, as provided through a figure in Raymer[11], it is slightly larger in magnitude. This is due to the upper surface blowing as is suggested by Keen and Mason[12]. As the aircraft increases in Mach, the pitching moment should grow in magnitude to approximately -1.30.

11.2. Lateral/Directional Stability

The second and third stability axes are the lateral and directional stabilities. The lateral stability controls the stability of the rolling moment. Due to the laws of physics, the rolling moment is always countered by the increasing lift on the rolling wing. This results in very little pilot interaction as when the aircraft starts to roll in a particular direction, the lift increases on that lowered wing and maintains the aircraft's stability. For this reason, a stability state for which the lateral axis is aimed to maintain is that of total stability.

The directional stability is the yawing axis that allows for the aircraft to realign itself with the flight path. If the aircraft is yawed out of the flight path angle, then slip can be produced. This is corrected with use of the tail rudder. To maintain directional stability, it is desired to have total stability about the directional axis.

The lateral/direction stability can be solved for through the use of a program called LDstab[13], developed by Grasmeyer. The LDstab program was designed to take a list of measurements that existed over the aircraft and calculate the stability and control derivatives as well as some engine out information which will be discussed in a later section. Using the data calculated by the LDstab program an overall stability of the aircraft can be found as well as an aid in solving for lateral/directional control surfaces (i.e., rudder). The sizing will be discussed in the following sections.

As far as the aircraft stability, it can be concluded that there is a desired total stability on the three axes. By obtaining this type of stability standard on the three axes it allows for the aircraft to be able to maintain an overall stability that it keeps without much pilot intervention, as well as allowing the pilot to have a decent amount of maneuverability without requiring him to overpower the cockpit controls.

11.3. Control Surface Sizing

The S.T.O.R.K. was been designed for upper surface blowing, to aid in our goal of creating a STOL aircraft. This upper surface blowing system does not work, however, without the assistance of specifically designed flaps. For our design, we have chosen to use USB (Upper Surface Blowing) Flaps behind each of the four engines. Each engine will have an individual flap that will allow the pilot to have complete control of each flap as needed. The USB flap works by having the channeled bled air from the engine as well as the natural flow of air over the airfoil, guided into the double flap system which creates higher lift at lower speeds. This will allow our aircraft to reach the lift goal necessary to take off within our set runway distance without having to reach “normal” speeds for such a lift. In Figure 11.1, below, a representation of how upper surface blowing works is illustrated.

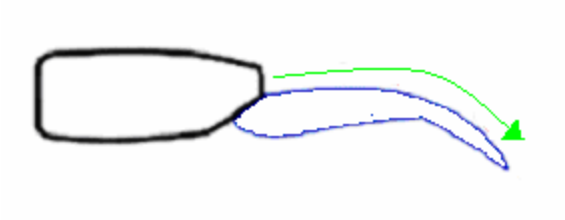

Figure 11.1 Upper Surface Blowing over the USB flaps

To aid in the attachment of the airflow over the flaps there are vortex generators that are located on the upper surface of the wing. On each of the USB flaps there are four vortex generators. They extend fully during low speeds to help the flow stay attached longer and increase lift. During cruise the vortex generators retract with the flaps. The USB flaps can range in extension angles between 0 degrees (fully retracted) to almost 90 degrees (fully extended). The USB flaps are each approximately 6.5% of the wing span (4.72 ft long) and 32% of the chord (5.60 ft wide).

Below is a depiction of the airfoil with the double slotted flap system fully extended, as well as the Krueger flaps fully extended on the leading edge.

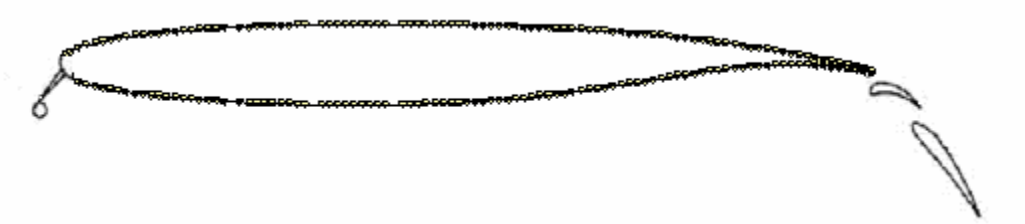

Figure 11.2 Airfoil with extended Krueger flaps on the leading edge and the double slotted flaps on the trailing edge (Krueger flap and double slotted flaps added to teams airfoil)[14].

Double-slotted flaps have been chosen to be positioned to the outside of either USB flap groups. Each of the two outer flaps comprises 20% of the total trailing edge wing span and 32% of the chord. This relates into a flap of length 14.5 ft by a width of 5.60 ft. On both outer trailing edges, there will be differential ailerons for aircraft roll. The differential ailerons will aid in any adverse yaw issues that may be encountered during the mission. The ailerons are each 17% of the trailing edge wing span and 18% of the chord. This translates to a length of 12.33 ft by a width of 3.17 ft. On the leading edge, Krueger flaps have been added to the design. Krueger flaps have the ability to aid in lift which is only a benefit to a STOL aircraft design. The leading edge

flaps have been designed to control 33.5% of the leading edge wing span and between 5-8% of the chord to either side of the engine sets.

Sizing for the elevators is performed in a similar manner. The elevators were each designed to control 45% of the trailing edge on the tail and 40% of the chord. The elevators on either side of the tail were divided into an inner and outer elevator. This resulted in having two inner elevators and two outer elevators each 4.5 ft in length by 3.22 ft in width. The estimated control surface sizes are taken from suggestions provided by Raymer[15].

The lateral/directional surface control sizing, that is the sizing of the rudder, is found by solving the yawing moment that results from asymmetric flight conditions. These calculations allow for a sizing of the rudder that would enable the pilot to maintain control of the aircraft in a "worst case scenario" situation, such as a single engine out. In a case such as the single engine out, Etkin and Reid[16] suggest that the rudder should be sized using the following equations.

$$C_n = C_{n_\beta}\beta + C_{n_{\delta r}}\delta r + C_{n_T} \tag{11.11}$$

$$C_{n_T} = \frac{-Ty_p}{\frac{1}{2}\rho V^2 Sb} \tag{11.12}$$

$$C_{n_{\delta r}} \le -\frac{C_{n_T}}{(\delta r)_{\max}} \tag{11.13}$$

It is equation 11.13 that is the necessary parameter to follow to create a rudder large enough to overcome the single engine out scenario. In equation 11.11 we want β to be zero and the overall yawing moment to be zero so as to achieve equilibrium.

Using the results from the LDstab program, which was discussed earlier, as input to a program titled VCMA[17] (also developed by Grasmeyer), rudder size estimation can be calculated. The VCMA program was designed to output, among other things, the rudder deflection. Using this information, as well as the other information calculated with the Grasmeyer programs, an estimated constraint list can be developed. With the calculated restraints found from the single engine out program, in addition to suggested rudder sizing from Raymer[18], a rudder area of 77.63 ft^2 is found. In the Figure 11.3, the rudder sizing can be seen in the vertical tail layout.

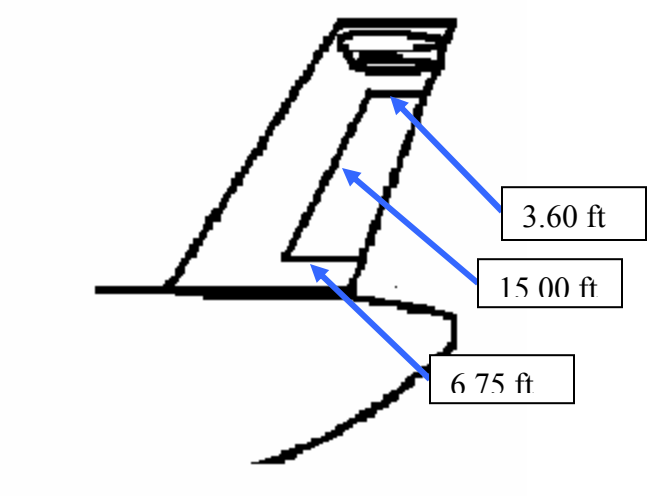

Figure 11.3 Rudder Dimensions

11.4. Flight Control System

For the pilot to be able to maneuver the aircraft in any desired way, it is necessary for there to be a well designed flight control system. The control system is comprised of cockpit controls which have connecting linkages (whether they are mechanical or electrical) that translate directional signals to the control surfaces. These control surfaces are composed primarily of the ailerons, the rudder and the elevators. These three components aid in maneuvering the aircraft through pitch, roll and yaw. On the S.T.O.R.K., it has been implemented that to reduce the number of control instruments in use by the pilot there will be a single control yoke which will link to the ailerons and the elevators. This single yoke will control the roll and pitch of the aircraft.

All of the cockpit controls and control surfaces have to have a link system that relays the information given by the pilot to the actual mechanism that controls the control surface. There were many methods of link systems researched for this design, such as a mechanical and a fly-by-wire (FBW) system. From the RFP, it is stated that there is a STOL requirement on the aircraft. This hinders the kind of weight that the aircraft can take on. It is also stated in the RFP that there will be a 60,000 lb payload, which requires that in the design of the aircraft there be as little weight addition as possible. For this reason, the design team has chosen to install a digital fly-by-wire system. The FBW control system far under weighs that of the mechanical system. A

lighter system poses greater benefits to the STOL requirement. There is also a less complicated system of computers used by the FBW system, which reduces the large cables and difficult routing of such cables throughout the body of the aircraft. In addition, the FBW has more advanced technology, which pushes the aircraft design into a more advanced position. By having the newer technology onboard the aircraft, it only reduces the work on the pilot and creates a safer and more responsive vehicle. This allows for the military to be at an advantage in hostile settings.

The digital fly-by-wire system is an advanced computer based control system. This system allows for a more stable and maneuverable aircraft. This is accomplished through a serious of computers which are constantly receiving inputs from all over the aircrafts control surfaces. There is a great needing for multiple computer back ups on aircrafts with digital fly-by-wire. This is due to the fact that the computer is the only link to the flight control surfaces, and if there is a failure in the computer system, all controls are lost. The multiple computers back up increases the price of the fly-by-wire system.

The digital FBW system was felt to best fit the design task set forth by the RFP. The digital system would allow for the pilot to have the best maneuverability as well as a faster and more specific response system. The technology will allow for the aircraft to maintain usability and desirability for a greater length of time and the cost was within reason and justified for the overall design.

12. Propulsion

An important aspect in the design process was designing a propulsion system. Many other aspects of the design directly follow from parameters determined by the propulsion system. To name a few, the propulsion system and the fuel required to power it make up a very large fraction of the non-payload weight of the aircraft. Also, the thrust and the thrust to weight ratio are important parameters in determining the aircraft performance. In the design of a propulsion system, there are certain aspects that needed to be determined. These include the type of engines, number of engines, engine mounting type, and the thrust provided after installation. These topics are the focus of this section.

12.1. Engine Mounting

The first aspect determined in the design process was the engine mounting type. Early in the design process it was determined that the design would incorporate upper surface blowing (USB) to achieve the high lift coefficients that were expected to be required to take off in the specified distance. Two of the initial concepts were based on upper surface blowing. One of them used a nacelle type design while the other had the engines partially embedded in the upper surface of the wing. Aside from simply appearance, all of the advantages seemed to side with the nacelle design.

First, the nacelle design allowed the choice of using a medium bypass turbofan as opposed to being locked to the low bypass turbofan with the embedded design. The discussion on engine type will explore this aspect in greater detail. Second, all previous upper surface blowing prototype aircraft used nacelle type engine mounting. It was unclear what effect embedding the engines would have on the positive effects demonstrated by these aircraft. Finally, mounting the engines in nacelles allows the engine inlet to be placed ahead of the wing leading edge giving it access to undisturbed free stream air.

12.2. Number of Engines

The next aspect determined was the number of engines. One of the initial USB concepts used 2 engines, the other used 4 engines. It is possible to fulfill the thrust requirements of the design using 2 larger engines or 4 smaller ones; however there are other effects that must be taken into

consideration. These generally include engine cost, fuel consumption, weight, and engine out configurations. While 2 engines is generally more cost effective, lighter, and can be more fuel efficient, USB introduces very specific concerns when it comes to engine out configurations. Typical 2 engine aircraft (without USB powered lift systems) are limited in their engine out configurations by the rudder control power required to counteract the asymmetric thrust. This is not usually a problem, as the rudder control power needed is generally within a reasonable range.

When USB is introduced, the loss of the engine on one wing also results in a huge disparity in lift over each wing and thus a very large rolling moment. This rolling moment is well outside the range that could be counteracted with a simple aileron deflection. The only option then is to forfeit the USB powered lift benefits on the other wing, requiring significantly higher takeoff and landing airspeeds. In a potential combat environment, not only is being stranded by too short a field length not an option, but the risk of engine failure is significantly increased by either enemy fire or austere conditions. Therefore, this engine out condition would be unacceptable for a military aircraft.

This brings up two possible solutions. The first would be to somehow link the fan shafts of the two engines to allow the remaining engine to turn the fan of the failed engine as well as its own. The hope here is to provide enough thrust out of the failed engine to allow the USB powered lift to be used on both wings with minimal aileron correction. Any system to link the shafts would be quite complex, especially on a large aircraft where the engines would be necessarily far apart. It also assumes that the failed engine is intact enough that turning the fan shaft would actually provide thrust. Unfortunately, an engine that has undergone a “combat induced” failure is not likely to be intact enough to provide thrust from the fan. This solution is not only unnecessarily complex, it also raises survivability issues that are unacceptable for a combat aircraft.

The second solution is simply to use 4 engines rather than 2. While this option is more expensive and burns more fuel, it allows USB powered lift to be used even in the event of a single engine failure. In this case the loss of one engine does not result in nearly as large a difference in lift and keeps the required aileron correction manageable. The 4 engine configuration does this without the need for complicated and expensive linkage systems that would be another potential failure point. For these reasons, the final design will have 4 engines.

12.3. Engine Type

The next aspect of the propulsion system to de determined was the type of engine. The AMC-X engine decks provided by the AIAA provided the starting point for the engine type. The engine decks provided data for both a low bypass turbofan and a medium bypass turbofan engine. This data provides a good starting place and can be scaled up or down by as much as 20 percent. As mentioned earlier, the nacelle mounting allows for the choice between the medium or low bypass turbofan. The medium bypass engine keeps the fan and core flows separate through the separate exits for each and so cannot be embedded in the aircraft. The low bypass engine is a mixed flow design that mixes the fan and core flows within the engine and passes them through a single nozzle, allowing this engine to be embedded in the aircraft fuselage or wing. Since the design configuration chosen earlier uses nacelle mounted engines, either the low or medium bypass engine would be acceptable. The low bypass turbofan has a bypass ratio of 2 and can provide higher net thrust than the medium bypass turbofan, especially at lower altitudes and higher mach numbers as shown in Figure 12.1. Note that the following two Figures comparing the two types of engines show un-scaled thrust and fuel consumption data and are useful for comparison only. These Figures do not reflect the final thrust of the actual engine to be used.

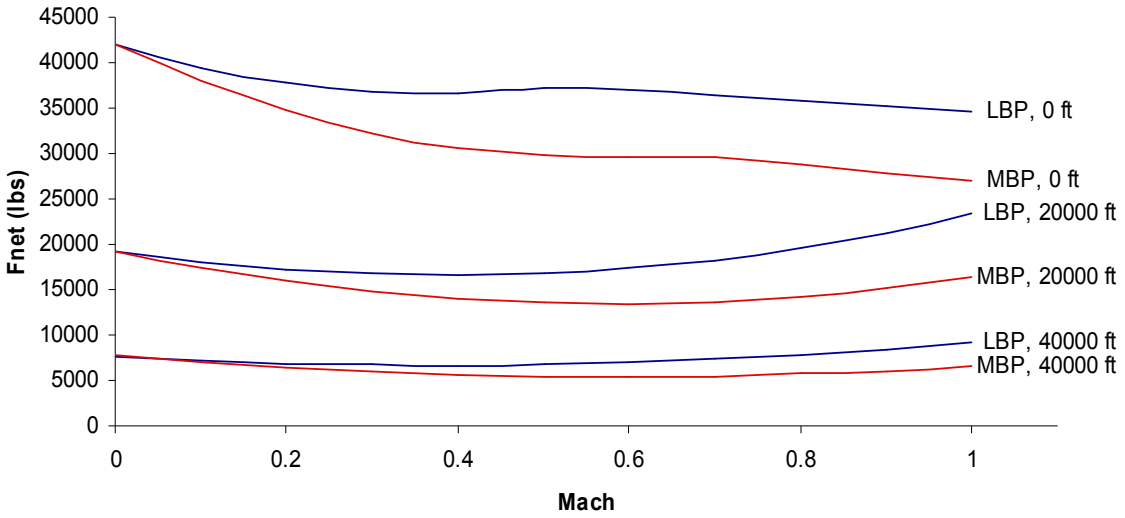

Figure 12.1 Thrust vs. Mach for Various Altitudes

Unfortunately, this thrust advantage comes at a steep price. Figure 12.2 shows that the medium bypass engine, with a bypass ratio of 6, has significantly lower thrust specific fuel

consumption than the low bypass engine. The difference is most pronounced in the region above Mach 0.8 where the aircraft must be designed to cruise. An added benefit of using 4 engines rather than 2 is that the increased thrust per engine from the low bypass engine is less important. As a result, the thrust advantage of the low bypass engines can be traded for the higher fuel efficiency of the medium bypass engines.

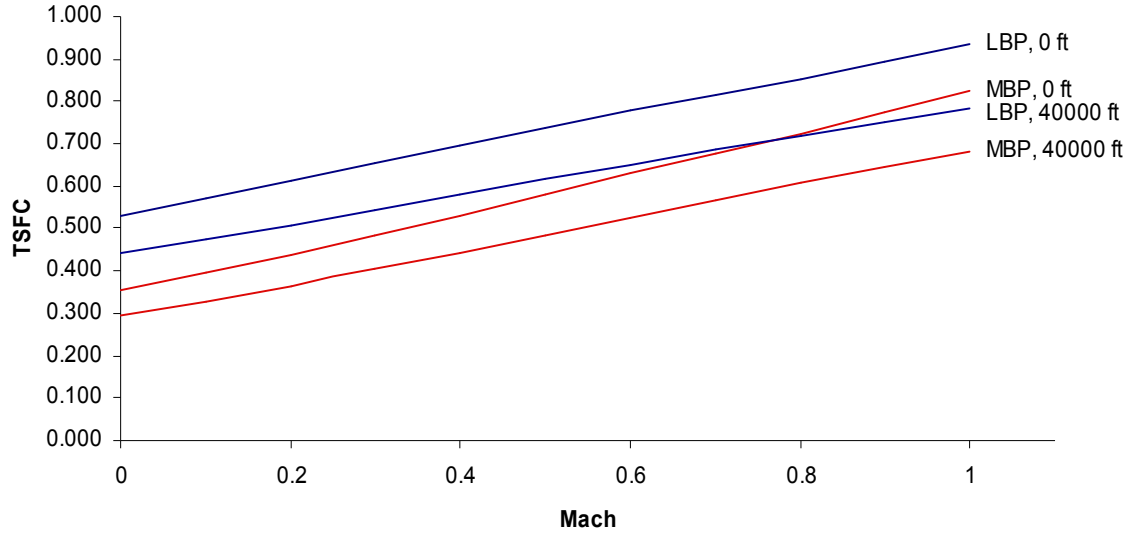

Figure 12.2 TSFC vs. Mach

12.4. Installation Effects

Once the engine type is determined, the next step is to determine the effects of installing the engine on the net thrust provided. The method that will be used here comes from Raymer chapter 13. This process is significantly simplified by the fact that the entire flight regime is subsonic. The thrust loss due to pressure losses in the inlet is given by equation 12.1. The reference pressure ratio is the inlet pressure ratio assumed by the manufacturer when calculating the uninstalled thrust data and for subsonic flight is generally taken to be 1.0. The actual pressure ratio for a subsonic nacelle configurations relatively low because of the very short duct. For this analysis the pressure recovery ratio is taken to be the worst case of 0.98. In equation 10.1, the C_{ram} term is the ram recovery correction factor and should be provided for various flight configurations by the engine manufacturer. In the event that it is not provided, Raymer states that it can be approximated as 1.35 in subsonic flight.

$$\%\ \text{thrust loss} = C_{ram}\left[\left(\frac{P_1}{P_0}\right)_{ref} - \left(\frac{P_1}{P_0}\right)_{actual}\right]\times 100 \qquad (12.1)$$

Once the inlet pressure drop losses are calculated, there are also losses due to bleed air that must also be taken into consideration. Bleed air can be taken from within the compressor to provide high pressure air for cabin pressurization, powered lift, and other aircraft systems. The engines chosen for this design have up to 5 percent of the total engine intake mass flow available for bleed air. This bleed air, while useful, more than proportionally decreases the engine thrust according to equation 12.2. The bleed correction factor, C_{bleed}, should be provided by the manufacturer, but in the event that it is not, Raymer states that it can be approximated as 2.0. Since this aircraft is not going to have any internally blown powered lift systems requiring bleed air, the bleed air will primarily be used for cabin pressurization. The bleed air mass flow will be assumed to be 2%.

$$\%\ \text{thrust loss} = C_{bleed}\left(\frac{bleed\quad massflow}{engine\quad massflow}\right)\times 100 \qquad (12.2)$$

These are the primary factors that reduce the installed thrust for a subsonic nacelle design. Corrections for the installed net propulsive force that take into account the drag induced by integrating the engine into the aircraft include spillage drag, bypass drag, boundary layer bleed drag, and nozzle drag are unique to either supersonic speeds or embedded configurations and can be considered negligible for a subsonic nacelle.

12.5. Engine Scaling

As stated earlier, the provided AIAA engine deck can be scaled up or down by as much as 20% of the gross uncorrected thrust. These base values need to be scaled to provide the appropriate level of thrust. The engines must provide enough thrust for takeoff as well as enough thrust to cruise at the required Mach 0.8. Based on tests using the mission analysis program and the takeoff program, the engines provided the necessary thrust while requiring the least fuel when scaled down to 90% of the original gross thrust. This gross thrust was corrected for installation effects as described in section 12.4. As scaled, the engines produce a maximum net sea level static thrust of 35,347 lbs each, for a total of 141388 lbs of thrust. Each engine weighs 7171 lbs, and is 121 inches long by 78 inches in diameter. The engines have a sea level static

thrust specific fuel consumption of .3793 based on installed net thrust, which corresponds to a full power fuel flow of 13407 lbs per hour for each engine.

13. Aerodynamics

13.1. Planform

One of the initial steps taken with regards to the aerodynamics of the aircraft was designing a wing planform capable of producing enough lift to get the aircraft off the ground. During cruise, the lifting force equals the weight of the aircraft. Using the weight of the aircraft and the planform area, one can find the lift coefficient using equation 13.1. The density was taken from the standard atmosphere tables at 35000 ft. The velocity was calculated using the cruise mach of 0.8 converted into true airspeed using the speed of sound at 35000 ft.

$$C_l = \frac{W}{\frac{1}{2}\rho V^2 S} \tag{13.1}$$

Using the planform area of 2280, the lift coefficient during cruise equals 0.65. The next step was acquiring the correct shape of the planform. Sweep and taper ratio can be altered to achieve the optimum shape. Using the Korn equation for transonic cruising speeds, one can iteratively use different values to get the correct geometry. Using equation 13.2 with a Mach divergence number (M_{DD}) of 0.82, a C_L equaling 0.65 and a K_A equaling 0.95 due to the use of a supercritical airfoil, the sweep equals 16.59 degrees with a *t/c* ratio of 0.085.

$$M_{DD}\cos\Lambda + \frac{t/c}{\cos\Lambda} + \frac{C_L}{10\cos^2\Lambda} = K_A \tag{13.2}$$

Figure 13.1 shows the aircraft's planform. Notice the taper ratio on this aircraft is 0.25. Raymer's airfoil and geometry section states that swept wings normally have a taper ratio between 0.2-0.3, therefore 0.25 was chosen.

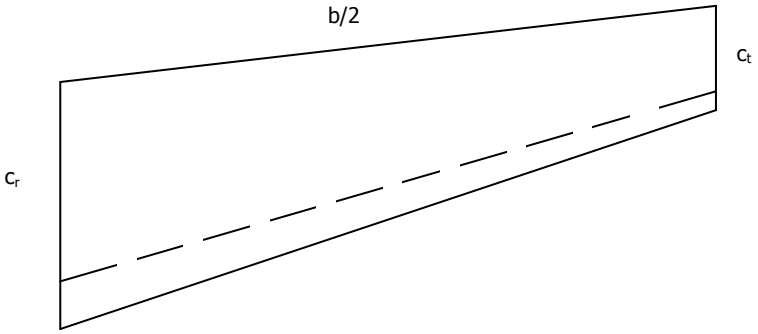

b/2 = 72.5	$\Lambda_{c/4}$ = 11.10°	t/c = 0.085
S = 2280	c_r = 25.16 ft.	λ = 0.25
AR = 9.22	c_t = 6.29 ft.	Λ_{LE}= 16.59°
MAC = 4.403 ft.	C_{bar}= 17.61 ft.	

Figure 13.1 Final Wing Geometry

13.2. Airfoil

The next step with regard to aerodynamics was to decide on an airfoil. To meet the AIAA requirements it was necessary for our aircraft to cruise at Mach 0.8. This presented a challenge due to it falling in the transonic speed range. A conventional airfoil presented issues when the speed reaches Mach 1. The air flowing across the top of the wing speeds up and passes the speed of sound. As a result, a shock wave is created on the upper surface of the wing. This shockwave causes the smooth upper surface flow to separate. This separation creates air that is turbulent and unsteady, resulting in drag increases. In extreme cases, this leads to the aircraft becoming uncontrollable due to the separation over the control surfaces. A solution to this effect was a created and tested in the early 1970s at the Dryden Flight Research Center. This airfoil was unconventional at the time and is now called a supercritical airfoil. A conventional airfoil is rounded on the upper surface and flat at the bottom. A supercritical airfoil is flatter on the top. This relatively flat upper surface doesn't accelerate the flow as much as the round conventional airfoil and therefore delays the shock wave creation. The delay results in a reduction in aerodynamic drag. A negative result from the flat upper surface is a reduction in lift. To combat this, the upper surface is more curved towards the trailing edge (NASA Dryden). This difference is noticeable in the airfoil geometry. (See figure 13.2).

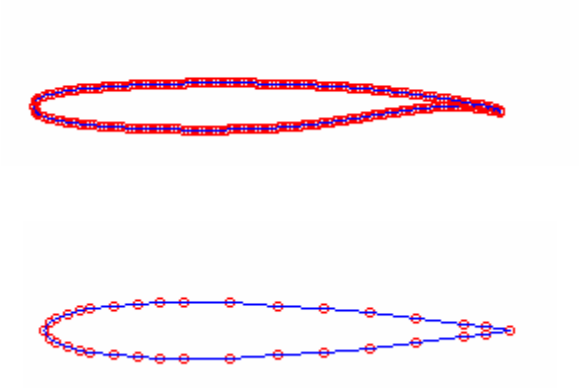

Figure 13.2 above) Supercritical airfoil Below) Conventional Airfoil

Take notice of the super surface of the conventional airfoil and how rounded it is compared to the upper surface of the supercritical airfoil. Also take note near the trailing edge of the supercritical airfoil. The added curvature makes up for the loss of lift from the flat upper surface. To verify the benefits of this effect, three airfoils were run through a transonic airfoil analysis program. TSFOIL2 is the program used, and it provides a finite difference solution of the transonic small disturbance equation. This program takes an input with the geometry of the airfoil, free stream Mach number, angle of attack, and various other parameters. It then outputs the lift coefficient, moment coefficient, and total drag coefficient. The three airfoils run through the program were the NACA 0012, NACA 2412, and the SC (2) – 0610 airfoil. The free stream Mach number is set at 0.85 and the angle of attack (AoA) is set at 0 degrees AoA. See the below table for the results of the program.

Table 13.1 Results of Running TSFoil 2 Program with 3 Airfoils

Airfoil	AoA (degrees)	C_l	C_d	C_m
NACA 0012	0	0.370532	0.119267	-0.307325
NACA 2412	0	0.622119	0.094546	-0.307325
SC(2)-0610	0	0.665154	0.053458	-.299737

The results of the program show that the C_d of the supercritical airfoil (SC(2)-0610) is much less than the C_d of the two conventional airfoils tested. It also shows that the C_l is also greater for

the supercritical airfoil than the two conventional airfoils. These results prove that the supercritical airfoil is the best type of airfoil

13.3. Strut

The S.T.O.R.K. requires the use of struts to support the wing. This presented another oddity in the aerodynamic characteristics of the aircraft. The point of interest was the intersection of the strut and the wing. At this point the flow accelerates creating a "channel-effect". This acceleration creates shockwaves, similar to the ones created using a conventional airfoil. In turn, these shockwaves create separation and an increase in interference drag (see figure 13.2 Tetrault, pg 79). This drag varies with the angle of intersection between the strut and the wing. The closer to 90 degrees the intersection angle is, the less increase in drag. Using this principle, an arch intersection is designed to increase the intersection angle (see figure 13.3, Tetrault, pg 77)

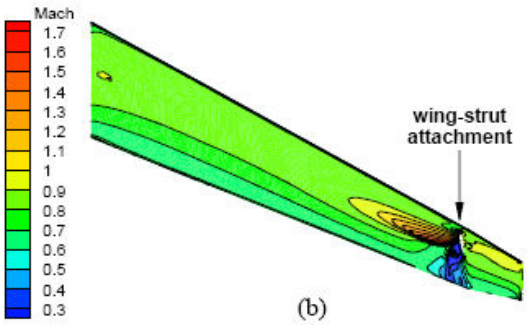

Figure 13.3 Acceleration at strut-wing intersection

(a) (b)

Figure 13.4 a) Intersection without arch b) Intersection with Arch

(Ref. Grasmeyer, Joel M.)

The increase in drag is shown below in table 13.2. As the radius of the arch increases, the change in drag decreases.

Table 13.2 Change in Drag as Radius of Arch Increases

Configuration	C_L	C_D	ΔC_D
Clean wing	0.5253	0.0121	0.0000
Arch with $R = 0$ ft (straight strut)	0.5396	0.0152	0.0031
Arch with $R = 1$ ft	0.5330	0.0147	0.0026
Arch with $R = 2$ ft	0.5308	0.0141	0.0021
Arch with $R = 3$ ft	0.5300	0.0137	0.0017
Arch with $R = 4$ ft	0.5282	0.0133	0.0013

(Phillipe-Andre Tetrault pg 83)

A balance between aerodynamic effects and structural effects needed be found to find the optimum radius of arch for the strut-wing intersection. Another benefit of adding a strut to the wing is the increase in allowable wing span. The increased wing span and reduction in weight reduces the induced drag. Also a smaller thickness to chord ratio (*t/c*) is allowed. A smaller *t/c* delays the shock which in turn decreases the wave drag. (pg 92-93 Grasmeyer)

13.4. Upper Surface Blowing

Upper surface blowing helps create lift at lower speeds. This is necessary to achieve the STOL requirements. Using the USB flaps it helps us achieve a C_{Lmax} of 4.96. This allows us to take-off from a shorter length runway because less speed is needed to generate that lift. With this

added lift comes added drag. The added drag is overcome by the four powerful engines. The drag is discussed in more detail in section 14.

13.5. Lift-Slope Curve

The next step was to calculate the lift-slope curve. Equation 13.3 in Raymer was used in the initial calculation. VLMpc is being tested using the same parameters to verify the results of equation 13.3 this equation is used and is accurate up to the same drag-divergent Mach number used above in the Korn Equation. It uses the aspect ratio A, max sweep, area exposed (S_{wxp}), reference area (S_{ref}), an airfoil efficiency (η). β, and a fuselage lift factor (F) See the equations below to see the complete analysis of the lift-slope curve.

$$C_{L_\alpha} = \frac{2\pi AR}{2 + \sqrt{4 + \frac{AR^2\beta^2}{\eta^2}\left(1 + \frac{\tan^2 \Lambda_{\max t}}{\beta^2}\right)}}\left(\frac{S_{exposed}}{S_{ref}}\right)(F) \qquad (13.3)$$

(Raymer 12.6)

AR = Aspect Ratio = 9.22
$B^2 = 1 - M^2 = 0.6$
η ≈ 0.95
$F = 1.07(1 + d/b)^2 = 1.488$
d = Fuselage Diameter
d = 12 ft.

$S_{exposed}$ = Area exposed = 1664 ft.sq.
S_{ref} = Ref. Area = 2280 ft.sq.
Λ = 11.10°

Using all these values, the lift-slope curve comes out to be 0.065 per degree. It is something to note that as the lift slope curve reaches C_{Lmax} it becomes near flat. The lack of a sharp drop off causes the stall characteristics to differ and be less noticeable than a normal aircraft. Sink-rate is something to keep an eye on when flying near C_{Lmax}.

14. Drag

14.1. Parasite Drag (Zero Lift Drag)

The next task was to calculate the drag of the aircraft. This was done on a component by component basis using the drag build-up algorithm stated in Raymer's Aerodynamic section. The first step is to calculate the parasite drag (C_{D0}). The component build up method is used, using equation 14.1.

$$(C_{D0}) = \frac{\Sigma(C_{fc} FF_c Q_c S_{wetc})}{S_{ref}} + C_{Dmisc} + C_{DL\&P} \qquad (14.1)$$

(Raymer 12.24)

C_{fc}= flat plate skin friction FF_c= Form factor

Q_c= interference factor C_{Dmisc} = flaps, gear etc.

$C_{DL\&P}$ = Leakages

Table 14.1 C_{D0} **Components**

Flight Phase	C_f	C_{Dmisc}	$C_{DL\&P}$
Take-off	0.00881	0.00833	0.00000398
Cruise	0.0228	0.0109	0.00000449
Landing	0.00881	0.00834	0.00000407

The flat plate skin friction is caused by the surface of all the components. The Form factor takes into account the viscous separation of each component. The interference factor calculates the interference effects. The leakage factor is 2-5 percent of the parasite drag. This takes into account the cracks and crevices along the surface of the aircraft. Each part of the parasite drag has its own equation.

14.2. Drag due to lift

Drag due to lift was the next drag component calculated, as seen in equation 14.2. The *K* factor is calculated using the aspect ratio and Oswald efficiency factor. The Oswald efficiency

factor takes into account the lift distribution of the wing. The closer to 1, the more elliptical the lift distribution is. See equations 14.2 and 14.3 used to calculate these values.

$$K = \frac{1}{\pi A \,\mathrm{Re}} \tag{14.2}$$

$$e = 1.78(1 - 0.045 AR^{0.68}) - .0.64 \tag{14.3}$$

The Oswald efficiency of this aircraft's wing is 0.77. Knowing this the *K* value can then be calculated. Once the *K* value is found, the drag due to lift is this *K* value multiplied with the C_L^2 at the given flight condition.

14.3. Drag caused by Upper surface blowing

The next factor is the upper surface blowing. Using the YC-14 test case, it was found that the C_D was increased by 0.015, during cruise, due to the interference drag caused by the engine wing intersection. However the drag coefficient was decreases by 0.002 as a result of the engine exhaust blowing over the wings.

Table 14.2 Aerodynamic Coefficients

Mission Stage	**C_{D0}**	**C_D**	**L/D**
Take-off	0.0310	0.623	5.85
Cruise	0.0340	0.0539	12.06
Landing	0.0253	0.325	4.83

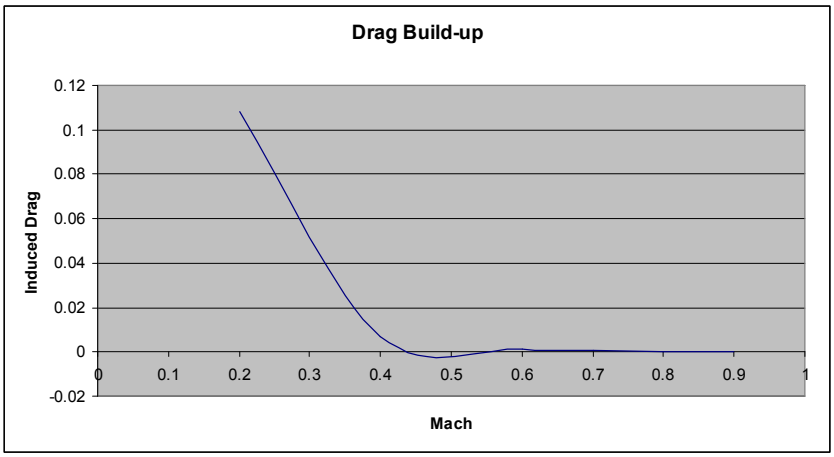

Figure 14.1 Drag Buildup

14.4. Drag Reduction

Several different methods can be used to reduce the drag even further. The easiest would be to add vortex generates on the upper surface of the wing. These may be as simple as little tabs placed on the upper surface to transform the laminar flow to turbulent flow. Another method is rounding off all the sharp intersections from each component of the aircraft. Smoother paint along the surfaces may also be used to lower the skin friction, hence lowering the drag. Below, figure 14.2 is the drag polar plot. The lowest drag coefficient coincides with the cruise lift coefficient of 0.65.

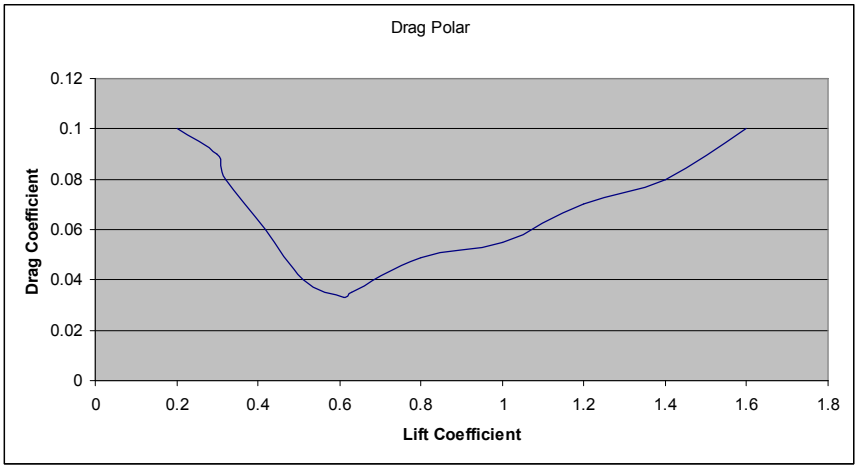

Figure 14.2 Drag Polar

15. Avionics

Communications is a huge part of a military aircraft's usefulness for its particular missions. The S.T.O.R.K. needed many types of communication devices. There is a VHF radio for basic communications between airports and other planes. In conjunction with the VHF radio the S.T.O.R.K. will also have a Secure Voice and Jam Resistant VHF/UHF/HF radio for security for communicating with military operatives. To satisfy its military qualifications, it will have an Identification of Friend or Foe or Selective Identification Feature. Without that equipment, the S.T.O.R.K. would not be able to operate in a hostile area, because of its inability to distinguish between friendly planes or enemy planes. Another important system the S.T.O.R.K. will employ is UHF Line of Sight equipment as well as Satellite communications capabilities. That will insure that the S.T.O.R.K. can see where it's going and be able to contact anyone that it needs to for its mission.

For navigation purposes the S.T.O.R.K. will have GPS system as well as Inertial Reference Units. Inertial reference units only account for radial acceleration so other systems will be needed to take into account the linear movement. There will also need to be UHF Direction Finding equipment. That system is needed to navigate through inclement weather during missions. To satisfy the all weather landing requirement, the S.T.O.R.K. will be equipped with Instrument Landing System and Marker Beacon. A VHF Omni-directional Radio beacon (VOR) and Distance Measuring Equipment (DME) is used on the S.T.O.R.K. missions. Another important component is a Weather Radar. With the weather radar, the S.T.O.R.K. can avoid storms that could cause damage.

The S.T.O.R.K. will be equipped with two HUDs, one for the pilot and co-pilot, as well as two smaller primary displays and one larger common multi-function display. The multi-function display would be used to display maps and other types of radar for use on the S.T.O.R.K.'s missions. There would also need to be mission computer and keyboards for each pilot and co-pilot to be used to get updated mission objectives while in flight. A very important instrument is the Warning and Caution System. The WACS is used to alert the pilots to any threat to the aircraft during flight. The final instrument needed for flight is an autopilot system for long continuous flights that would be monotonous and can be completed by the autopilot. Flights over

the ocean would be a prime example, there is no need for maneuvering and there are no threats over water.

Some additional systems that are needed are a Ground Proximity Warning System as well as a radar altimeter. The altimeter is used for normal in-flight instrumentation, while the ground proximity warning system is for alerting the pilot to his altitude when he is maneuvering near to the ground. The S.T.O.R.K. will also be equipped with a Flight Data Recorder, in case of inquiries into a crash or other such events as well as debriefing and mission success. There will also be landing gear controls, located on the center console for ease of access to each pilot. For controlling the aircraft, we have chosen the fly-by-wire technology because of its effectiveness and extensive use. Since it has been extensively used on other aircraft, there are not as many problems with this system as with newer systems such as fly by light. The S.T.O.R.K. will use two control yokes for the pilot and copilot stations, as well as common throttles on the center console.

16. Cost Analysis

A final measure of the adequacy of the S.T.O.R.K. in this design competition is the cost analysis. The 2006-2007 RFP did not present any cost constraints, and therefore the challenge faced by The Mason Project was to produce a transport which would meet all specifications for the least cost to the United States Air Force. Several methods were used to determine the final cost for the three production runs of 150, 500, and 1500 craft as posed by the RFP. Figure 16.1 shows the flyaway cost according to three different analysis methods with the vertical black lines indicating the three production runs. These methods are Raymer's modified RAND DAPCA IV Model[19] shown on the blue line, NASA Johnson Space Center (JSC) Cost Analysis based on a 2006 Cost Analysis Symposium[20] shown on the purple line, and finally an Aircraft Cost Estimation Methodology presented by J. Wayne Burns of Vought Aircraft Company[21] along the green line.

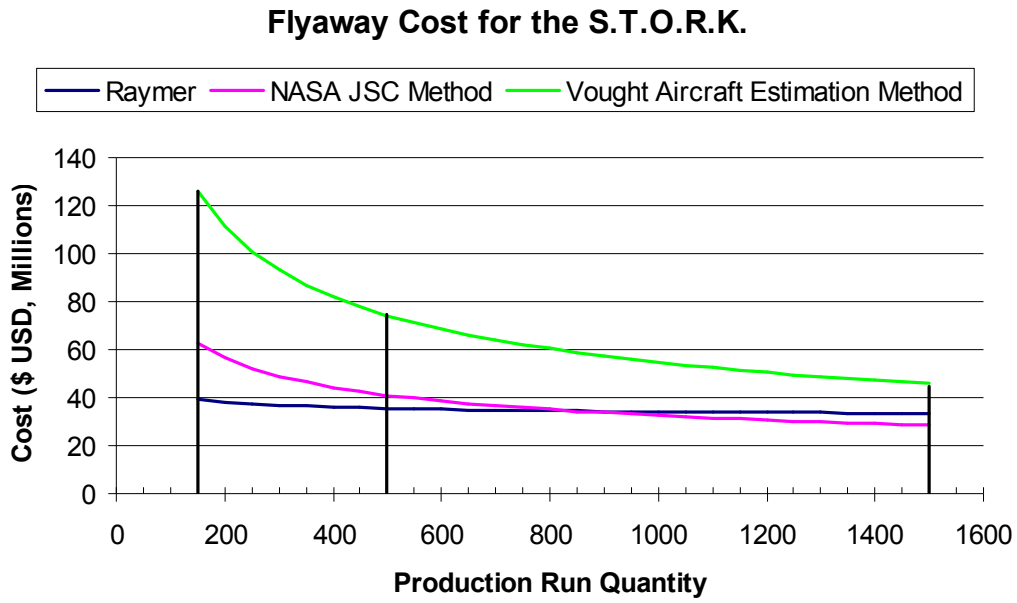

Figure 16.1 S.T.O.R.K. Flyaway Cost

Each method used required many of the same basic inputs such as airframe empty weight, maximum speed at cruise, fuel capacity and weight, and avionics weight and cost. Raymer's

method was the crudest approximation, and therefore the difference in cost between the smallest and largest productions runs was small. The NASA JSC method took into account more factors such as engine dimensions, number of engines, and type of missions being flown. This method started out with a mid-range cost of $62.6 million for the 150 production run and ended with the lowest cost of $28.6 million for the 1500 production run. The Vought Method for estimating was the highest overall, and took an over-estimation approach to the cost modeling. Most cost equations were based on weights and cost escalation factors which lead to a high initial cost of $76 million and a final last production run cost of $45.8 million. A comparison with the S.T.O.R.K. is presented in Figure 16.2 which shows the cost of similar aircraft at different production runs. As can be seen, using the NASA JSC data, the S.T.O.R.K. is consistently less expensive per craft than either the C-17[22] or the C-130 J[23]. With an average cost of under $40 million per aircraft for the 1500 production run, the S.T.O.R.K. rises above the competition as a cost-effective solution to the RFP.

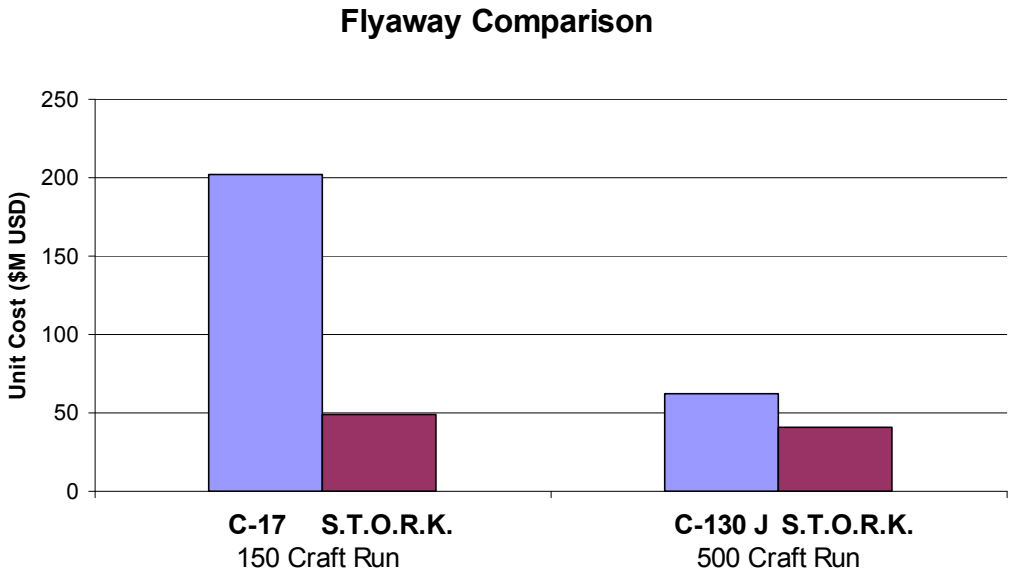

Figure 16.2 Flyaway Comparison Cost

Another factor which should be taken into account when determining the cost of an aircraft is the maintenance cost. A viable solution can be quickly negated by being too expensive to maintain over its service life. To determine the cost per flight hour, Roskam's Method for Estimating Operating Cost of Military Airplanes[24] was used. This method uses many of the same

factors as Raymer's, but also takes into account mission specifications and current $USD rates for payment in terms of salaries as well as fuel. The mission time, service life, and annual utilization hours were also factors in determining the cost per flight hour, which came to $13,967.20 for the 1500 craft production run.

Appendix

1. Concept Sketches

The following sketches are the three design concepts chosen to pursue as possible RFP proposal solutions.

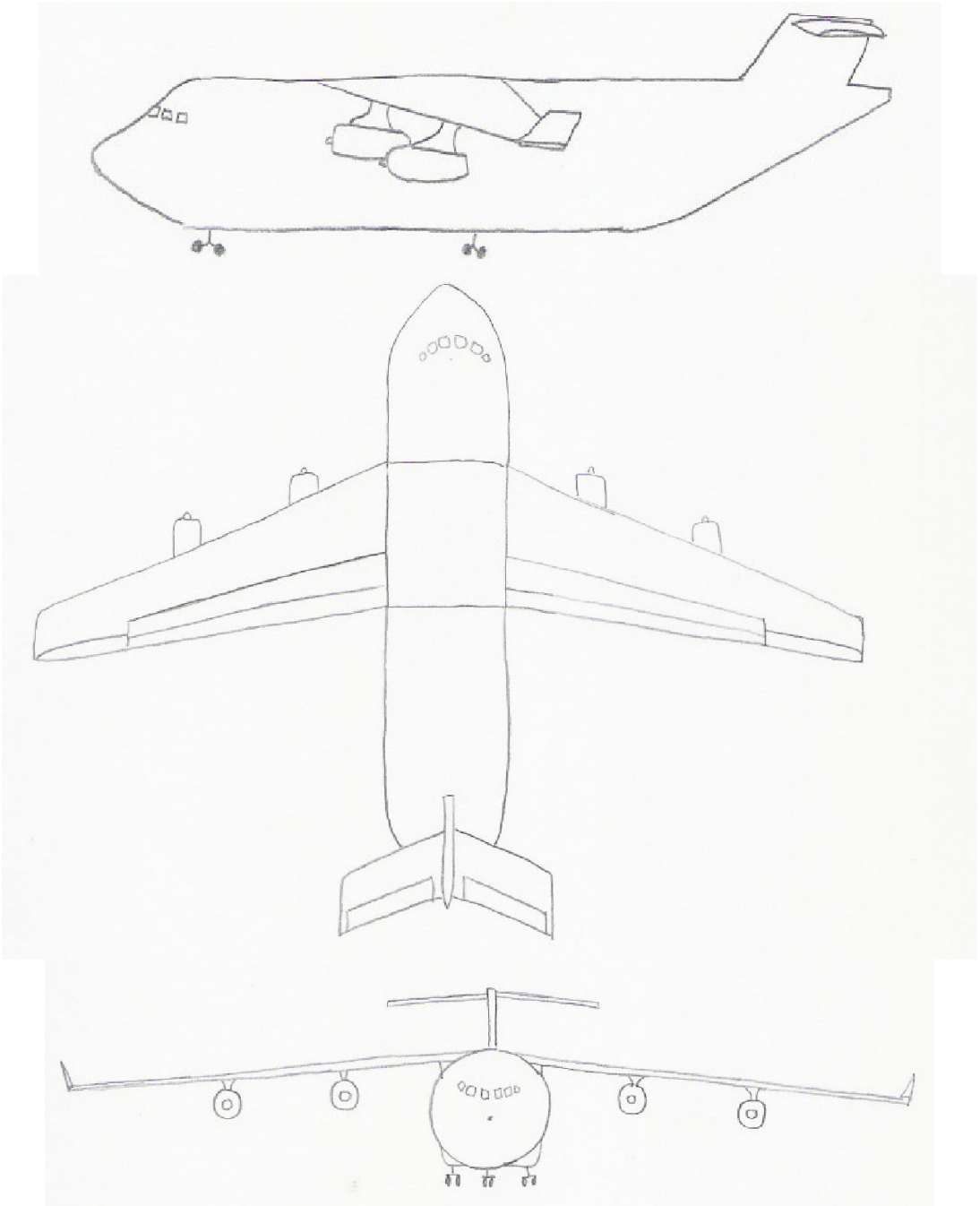

Figure A.1.1 Sketch 1

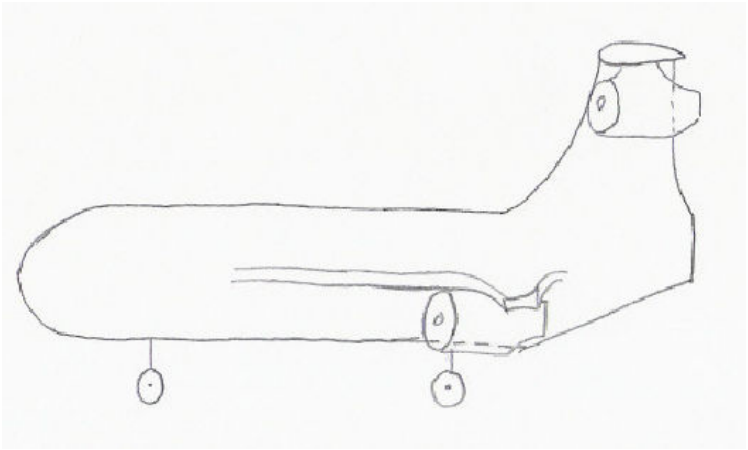

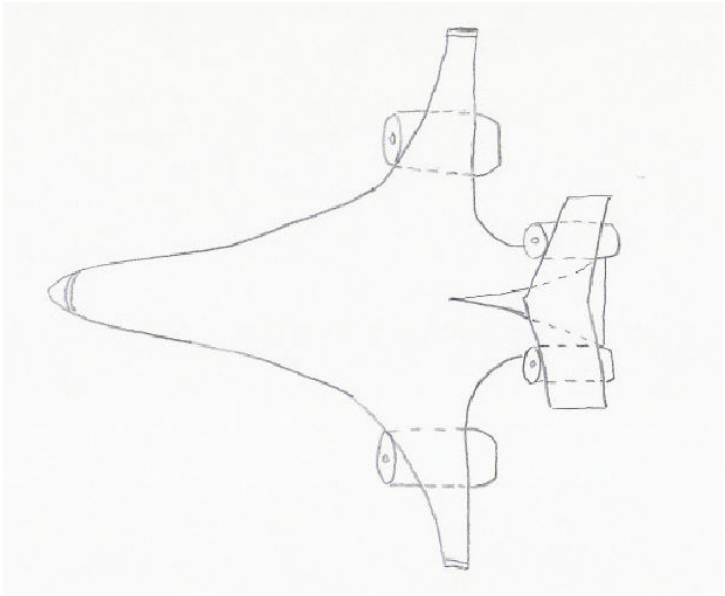

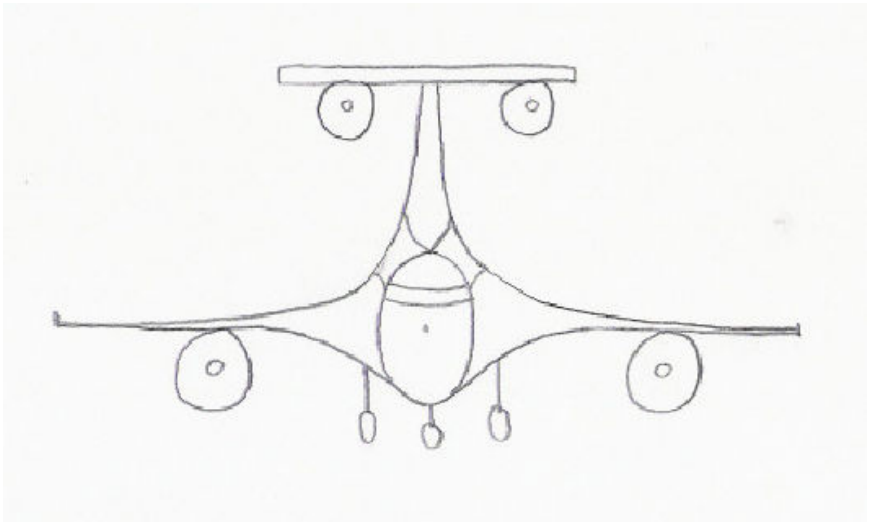

Figure A.1.2 Sketch 6

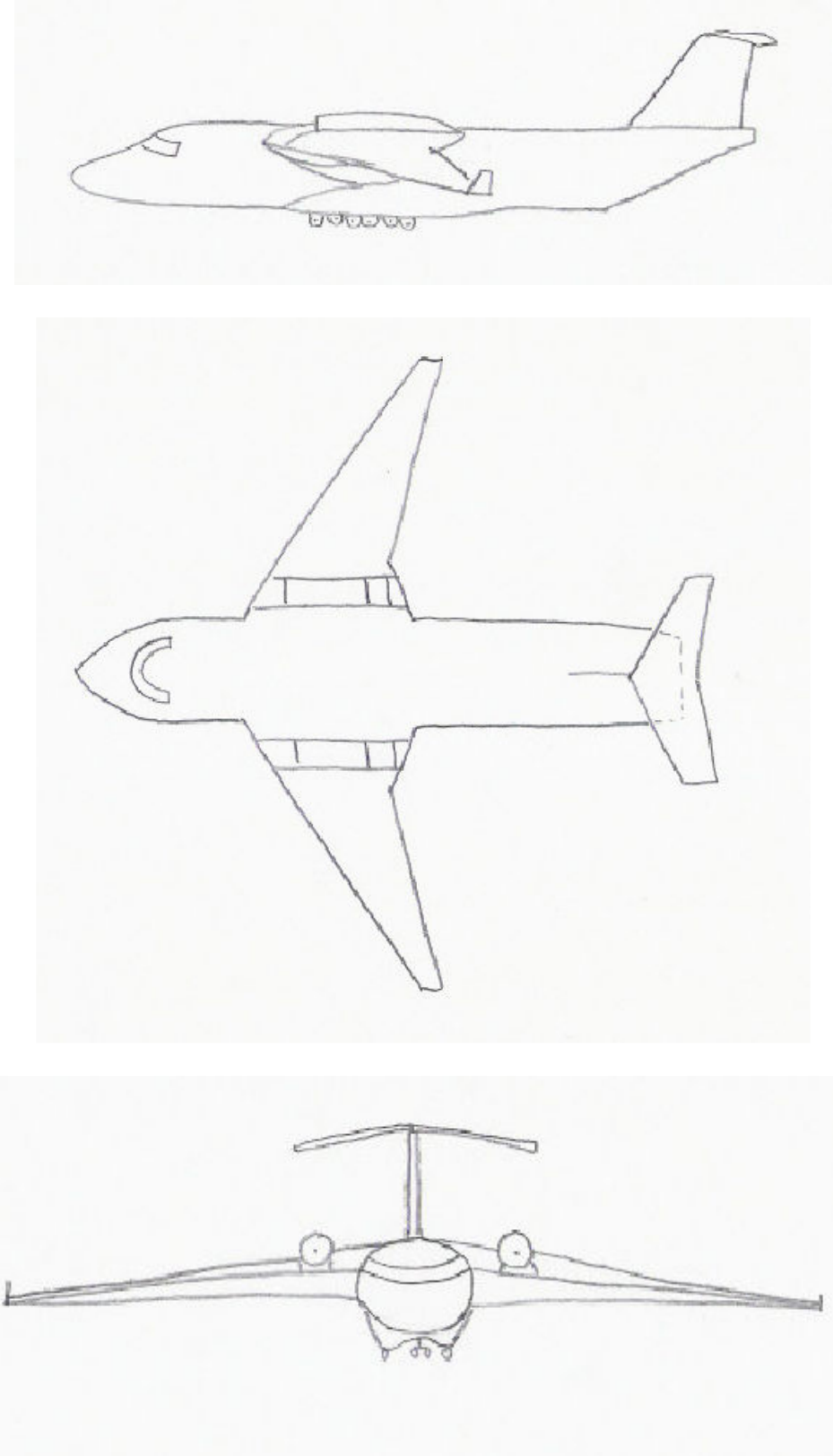

Figure A.1.3 Sketch 7

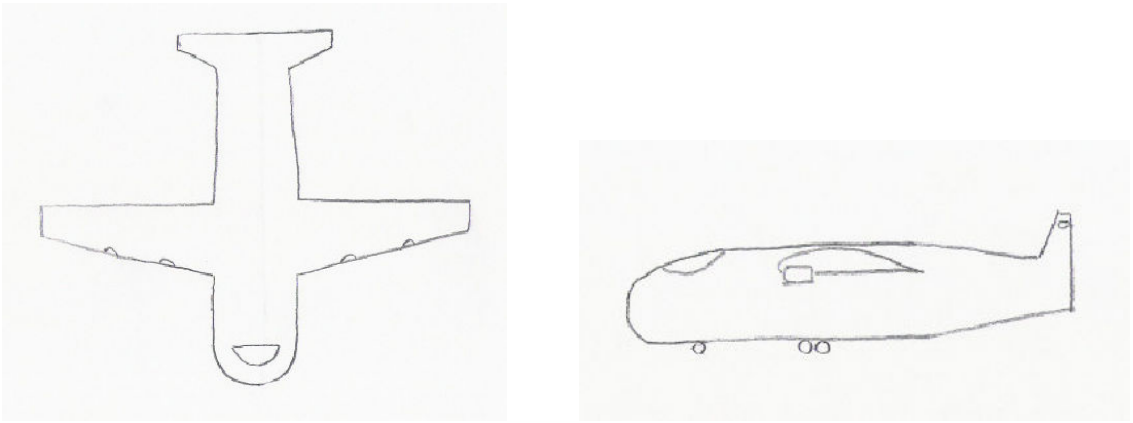

Figure A.1.4 Sketch Option 2

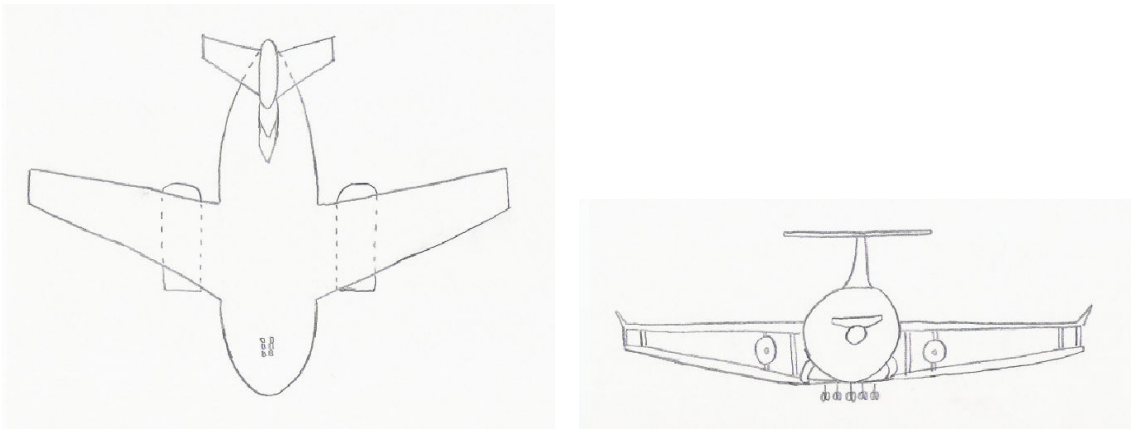

Figure A.1.5 Sketch Option 3

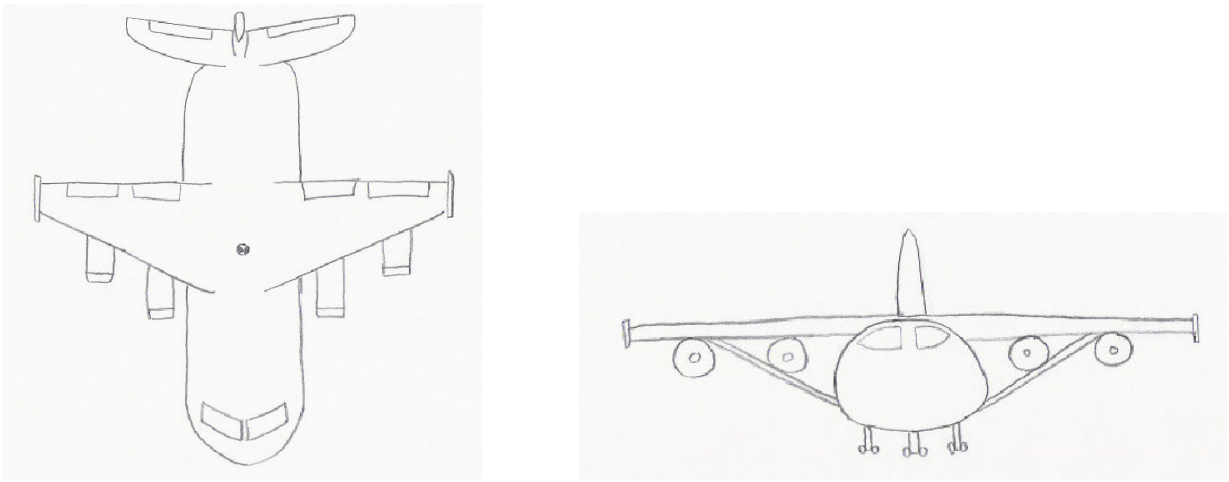

Figure A.1.6 Sketch Option 4

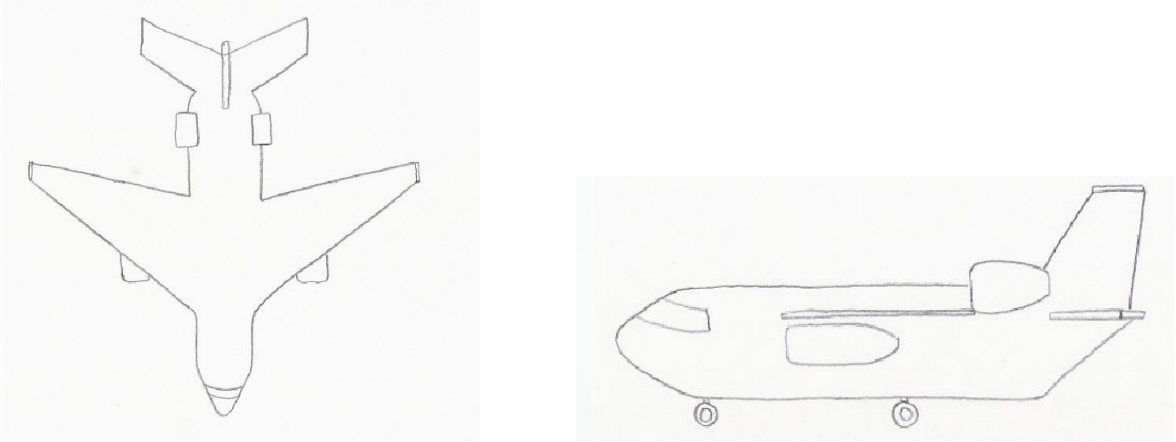

Figure A.1.7 Sketch Option 5

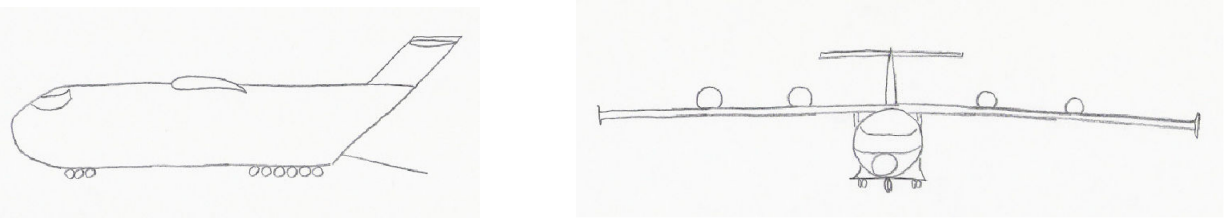

Figure A.1.8 Sketch Option 8

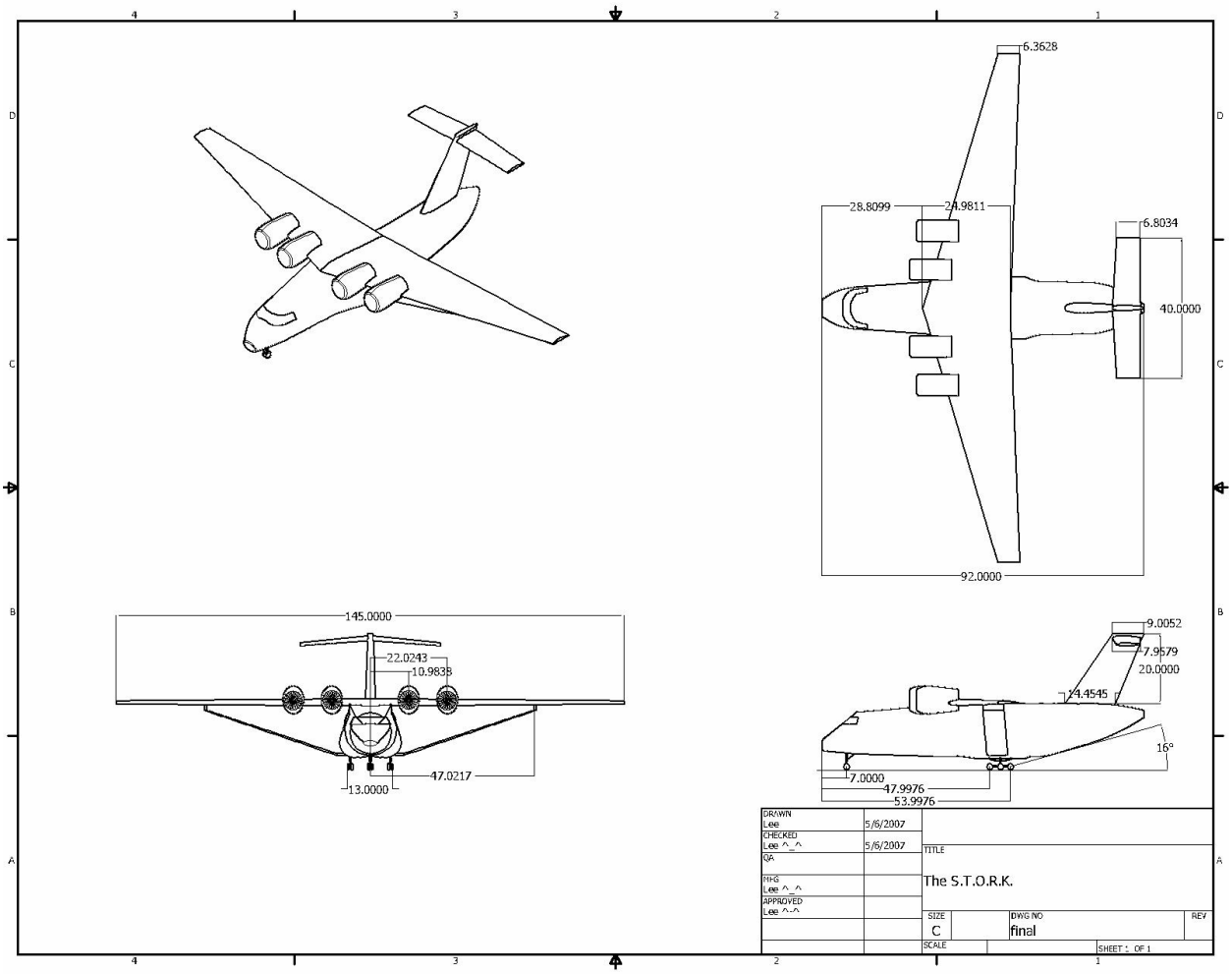

Figure A.1.9 The S.T.O.R.K. 3-View

2. References

[1] "Undergraduate Team Aircraft Design Competition." American Institute for Aeronautics and Astronautics. 2006. AIAA. <http://www.aiaa.org/content.cfm?pageid=223>.

[2] "C-130 Hercules." Wikipedia. <http://en.wikipedia.org/wiki/C-130>.

[3] "Boeing YC-14 N." Aviation Enthusiast Corner. <http://aeroweb.brooklyn.cuny.edu/museums/az/pam/72-1873.htm>.

[4] Naghshineh-Pour, Amir H. *Structural optimization and design of a strut-braced wing aircraft.* Blacksburg, Va. : University Libraries, Virginia Polytechnic Institute and State University, 1999

[5] Megson, T.H.G. *Aircraft Structures 3rd ed*. Burlington: ELSEVIER, 1999.

[6] Niu, Michael. *Airframe Structural Design*. Burbank, California. Conmilit Press. 1988

[7] Martin, Simmons. Model Aircrafts Aerodynamics. 4th ed. Vol. 1. Nexus Special Interests, 1999.

[8] Stoen, Hal. "A Weighty Issue. and a Balancing Act Too...." Stoenworks. 16 Jan. 2007. 5 May 2007 <http://stoenworks.com/A%20Weighty%20Issue.html>.

[9] Raymer, Daniel P. Aircraft Design: a Conceptual Approach. 4th ed. Vol. 1. Reston: American Institute of Aeronautics and Astronautics, 2006. 474-476.

[10] Etkin, Bernard, and Lloyd D. Reid. Dynamics of Flight: Stability and Control. 3rd ed. Vol. 1. Hoboken, NJ: John Wiley & Sons, INC., 1995. 23-28.

[11] Raymer, Daniel P. Aircraft Design: a Conceptual Approach. 4th ed. Vol. 1. Reston: American Institute of Aeronautics and Astronautics, 2006. 474.

[12] Keen, Ernest B., and William H. Mason. "A Conceptual Design Methodology for Predicting the Aerodynamics of Upper Surface Blowing on Airfoils and Wings." AIAA (2005): 1-15. 5 May 2007 <http://www.aoe.vt.edu/~mason/Mason_f/AIAA2005-5216.pdf>.

[13] Grasmeyer, Joel, comp. Stability and Control Derivative Estimation and Engine-Out Analysis. Jan. 1998. Department of Aerospace and Ocean Engineering, Virginia Polytechnic Institute and State University. 24 Apr. 2007 <http://www.aoe.vt.edu/~mason/Mason_f/LDstabdoc.pdf>.

[14] Dick, Steven J. "High Lift Systems." Technology of the Jet Airplane. Feb. 2007. NASA. 5 May 2007 <http://www.hq.nasa.gov/pao/History/SP-468/p272b.jpg>.

[15] Raymer, Daniel P. Aircraft Design: a Conceptual Approach. 4th ed. Vol. 1. Reston: American Institute of Aeronautics and Astronautics, 2006. 123-126.

[16] Etkin, Bernard, and Lloyd D. Reid. Dynamics of Flight: Stability and Control. 3rd ed. Vol. 1. Hoboken, NJ: John Wiley & Sons, INC., 1995.

[17] Grasmeye, Joel, comp. A MATLAB M-File to Calculate the Single Engine Minimum Control Speed in Air of a Jet Powered Aircraft. Jan. 1998. Department of Aerospace and Ocean Engineering, Virginia Polytechnic Institute and State University. 24 Apr. 2007 <http://www.aoe.vt.edu/~mason/Mason_f/VMCAUserMan.pdf>.

[18] Raymer, Daniel P. Aircraft Design: a Conceptual Approach. 4th ed. Vol. 1. Reston: American Institute of Aeronautics and Astronautics, 2006. 125.

[19] Raymer, Daniel P. Aircraft Design: a Conceptual Approach. 4th ed. Reston: AIAA, 2006.

[20] Cyr, Kelley. "Cost Estimating Web Site." NASA JSC Cost Estimating and Models Web Site. 21 Jan. 2005. NASA. 28 Apr. 2007 <http://cost.jsc.nasa.gov/index.htm>.

[21] Burns, J. Wayne. "Aircraft Cost Estimation Methodology and Value of a Pound Derivation for Preliminary Design Development Applications." S A W E Journal (1994): 46-66.

[22] "C-17 Globemaster III." Air Force Link: Factsheets. May 2006. USAF. 1 May 2007 <http://www.af.mil/factsheets/factsheet.asp?fsID=86>.

[23] "C-130 Hercules." Air Force Link: Factsheets. May 2006. USAF. 1 May 2007 <http://www.af.mil/factsheets/factsheet.asp?fsID=92>.

[24] Roskam, Jan. Airplane Design: Airplane Cost Estimation. Vol. VIII. Ottawa: Roskam Aviation and Engineering Corporation, 1990.